Hualapai Limestone Member of the Muddy Creek Formation: The Youngest Deposit Predating the Grand Canyon, Southeastern Nevada and Northwestern Arizona

GEOLOGICAL SURVEY PROFESSIONAL PAPER 1111

HUALAPAI LIMESTONE MEMBER OF THE MUDDY CREEK FORMATION: THE YOUNGEST DEPOSIT PREDATING THE GRAND CANYON, SOUTHEASTERN NEVADA AND NORTHWESTERN ARIZONA

Hualapai Wash—Type locality for the Hualapai Limestone Member of the Muddy Creek Formation.

Hualapai Limestone Member of the Muddy Creek Formation: The Youngest Deposit Predating the Grand Canyon, Southeastern Nevada and Northwestern Arizona

By WILL N. BLAIR *and* AUGUSTUS K. ARMSTRONG

GEOLOGICAL SURVEY PROFESSIONAL PAPER 1111

UNITED STATES GOVERNMENT PRINTING OFFICE, WASHINGTON : 1979

UNITED STATES DEPARTMENT OF THE INTERIOR

CECIL D. ANDRUS, *Secretary*

GEOLOGICAL SURVEY

H. William Menard, *Director*

Library of Congress Catalog-card No. 79-600142

For sale by the Superintendent of Documents, U.S. Government Printing Office
Washington, D.C. 20402

Stock Number 024-001-03222-8

CONTENTS

ILLUSTRATIONS

TABLE

HUALAPAI LIMESTONE MEMBER OF THE MUDDY CREEK FORMATION: THE YOUNGEST DEPOSIT PREDATING THE GRAND CANYON, SOUTHEASTERN NEVADA AND NORTHWESTERN ARIZONA

By WILL N. BLAIR and AUGUSTUS K. ARMSTRONG

ABSTRACT

The Hualapai Limestone Member of the Tertiary Muddy Creek Formation is exposed as erosional remnants in the Lake Mead area of southeastern Nevada and northwestern Arizona and at the base of the Grand Wash Cliffs in northwestern Arizona. Earlier investigators have considered that this limestone was originally deposited along with mudstone, claystone, and siltstone from interior drainage in a lacustrine environment. On the basis of an analysis of chert and of the observed occurrence of diatoms typical of estuarine conditions, we interpret the limestone as having been formed in marine or brackish waters. The presence of radiaxial fibrous calcite cementing algal oncolites in the Hualapai Limestone Member also indicates early marine sedimentation.

Siliceous rocks within the Hualapai Limestone Member exhibit the diagenetic sequence of biogenic opal to cristobalite to chert, which is characteristic of rocks deposited in a marine environment.

The Hualapai Limestone Member was most likely deposited in an estuary at the end of an embayment of the Gulf of California, which extended northward to the edge of the Colorado Plateau in the vicinity of Lake Mead.

INTRODUCTION

This paper presents information on the rock types and environment of the Hualapai Limestone Member of the Muddy Creek Formation. The Muddy Creek Formation has been considered to be an interior basin deposit by most workers (Longwell, 1928; Hunt, 1956; Lucchitta, 1967). We believe that there is good evidence for a marine or brackish-water origin for the Hualapai Limestone Member. The site for this kind of deposition would have been at the north end of an embayment of the ancestral Gulf of California or in an estuary at the north end of the ancestral gulf.

MUDDY CREEK FORMATION

The Muddy Creek Formation was named the Muddy Creek Beds by Stock (1921, p. 146–147) for exposures between Overton and Logan (now Logandale), Nevada. Longwell (1928, p. 90–96) renamed it the Muddy Creek Formation and (1936, p. 1423) lowered its base to include strata previously assigned to the underlying Horse Spring Formation. The formation is a complex deposit, largely basin and trough type, composed of conglomerate, sandstone, siltstone, mudstone, and crystalline precipitates. It interfingers and is overlain by volcanic flows at several localities. Its uppermost part is distinguished by the Hualapai Limestone Member, a widespread flat-lying unit. The Muddy Creek includes abundant salt and gypsum lenses and other indicators of aridity (Longwell, 1954). North of the Colorado River, near the head of Boulder Canyon (now under Lake Mead), the Muddy Creek Formation is largely gypsum, which in places is at least 90 m thick. Before the creation of Lake Mead, large beds and plugs of rock salt of Miocene and Pliocene(?) age were exposed in part of the Virgin Valley (Longwell and others, 1965). Moreover, the paleobasin of Red Lake, about 32 km south of Hualapai Wash, contains a minimum of 1,200 m of evaporites, mainly halite (Peirce, 1976, p. 328). This lake basin appears to have been largely filled by 10 m.y. ago, before the establishment of the Grand Canyon. Peirce (1976) believes that the halite of Red Lake is the same age as the Muddy Creek Formation.

HUALAPAI LIMESTONE MEMBER

C. R. Longwell (1936), in his study of the Boulder Reservoir floor of Arizona and Nevada, named the Hualapai Limestone for the excellent limestone exposures along Hualapai Wash, its type locality.

Lucchitta (1972, p. 1939) considered the Hualapai to be the highest and youngest member of the Muddy Creek Formation. This usage was adopted by Blair (1978).

The Hualapai Limestone Member crops out in the northwestern part of Arizona, south of Lake Mead in Mojave County and in southeastern Nevada, north of Lake Mead in Clark County (fig. 1). It is exposed as

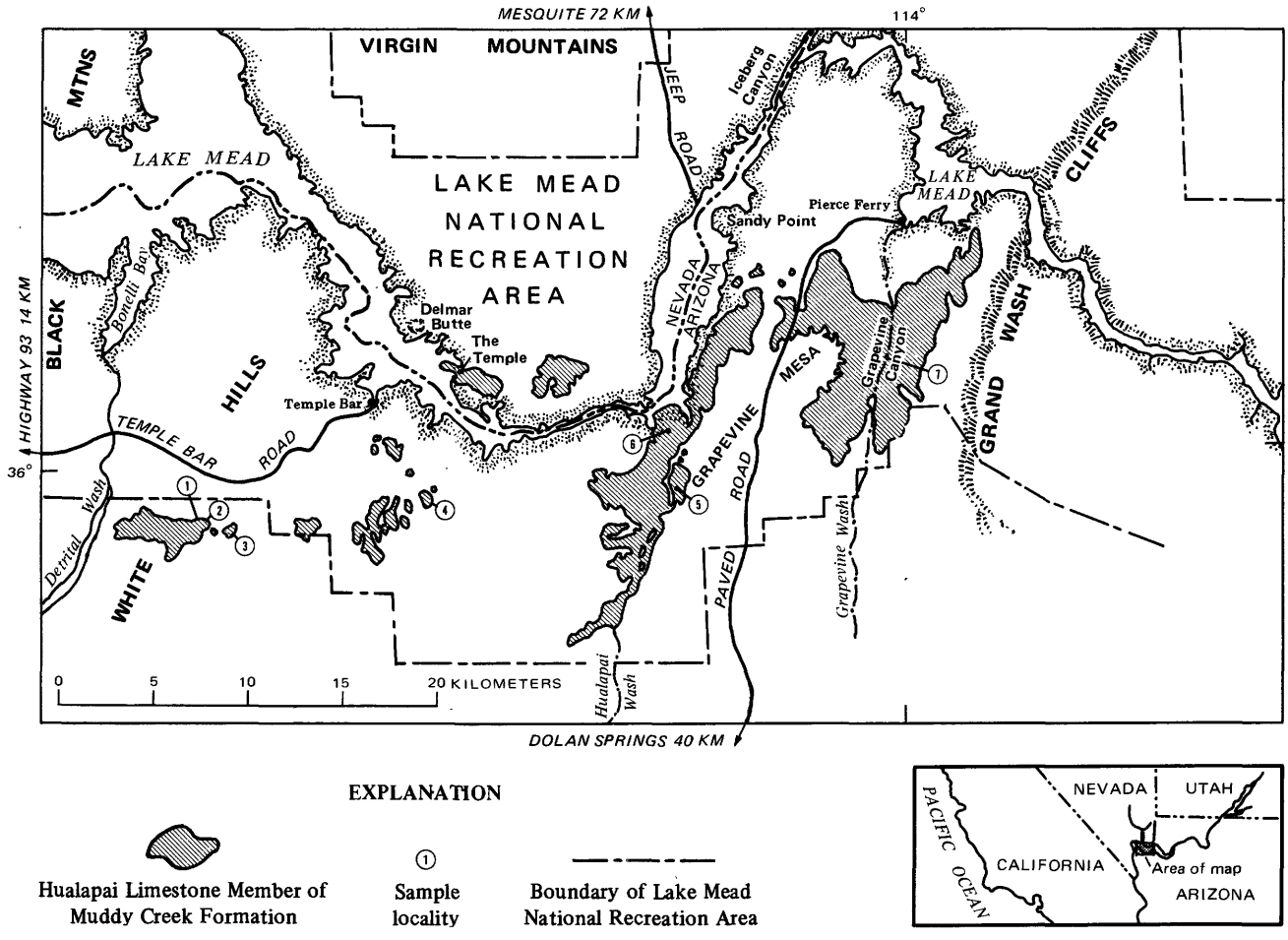

FIGURE 1.—Southeastern Nevada and northwestern Arizona showing distribution of Hualapai Limestone Member.

erosional remnants astride the present course of the Colorado River at the base of the Grand Wash Cliffs in northwestern Arizona.

Ancestral Colorado River gravel is found in siltstone conformably overlying the Hualapai (Blacet, 1975); however, nowhere in the Hualapai is there evidence of a vigorous through-flowing stream such as the present Colorado River. Therefore, the Hualapai Limestone Member probably is one of the youngest deposits formed before the establishment of the Colorado River in its present course from the mouth of the Grand Canyon.

DISTRIBUTION

Outcrops of the Hualapai Limestone Member occupy topographic lows that are generally bounded on the west by the Black Mountains and on the north by the Virgin Mountains (fig. 1). The White Hills form an approximate boundary to the south. To the east the Hualapai is bounded by the Grand Wash Cliffs, which form a steeply eroded fault scarp across the present course of the Colorado River where it emerges from the Grand Canyon.

The best exposure and the type locality of the Hualapai Limestone Member is along Hualapai Wash, beginning from the point where the wash joins Lake Mead and extending south for about 9 km (fig. 1). Here the Hualapai is over 240 m thick. A thick section of the Hualapai is also well exposed for about 2 km in steep cliffs along Grapevine Wash, about 8 km south of Pierce Ferry.

A third remnant, smaller than the first two, lies exposed near Detrital Wash, 8 km southwest of the Lake Mead marina at Temple Bar. Across the lake, smaller and thinner limestone beds cap Delmar Butte, The Temple, and an area just north of Iceberg Canyon.

Large exposures of the Hualapai to the south of Lake Mead can easily be reached by a paved road to Temple Bar from Highway 93, and by another paved road through Dolan Springs to Pierce Ferry. This road also departs from Highway 93 but further to the south.

Exposures of the Hualapai Limestone Member on the north shore of Lake Mead can be reached by a jeep

road from Mesquite, Nev., through the Virgin Mountains, a distance of some 72 km. However, a short boat ride across the lake from the Temple Bar marina will bring one to within easy walking distance of the Hualapai on the north shore.

The easternmost exposures of the Hualapai Limestone Member are those south of Pierce Ferry. They extend northward up Gravevine Wash for 12 km, roughly paralleling the Grand Wash Cliffs (fig. 2). Here the Hualapai rests conformably on and interfingers with conglomerate of the Muddy Creek Formation. The thickest unit is in Grapevine Wash where it forms rugged and steeply dissected cliffs, in contrast to the softer clayey limestone near the Pierce Ferry airport where the beds thin to about 60 m. The Hualapai and the conglomerate cover the Grand Wash fault, the exact location of which is unknown. There has been no movement on this fault during the last several hundred meters of deposition of the Muddy Creek.

The westernmost exposure of the Hualapai Limestone Member is 8 km south of Bonelli Bay (fig. 1) at a point on the east edge of Detrital Wash; it extends eastward from there for about 5 km. The Hualapai at this locality measures over 120 m and dips 5° to the east (fig. 3). The Hualapai overlies 6 m of massive gyp-

FIGURE 3.—Westernmost exposure of the Hualapai Limestone Member from locality 1 (fig. 1): (1) marl bed with fossil plants, (2) 8.66-m.y.-old tuff, (3) bed with radioactive material, (4) gypsum bed at the base of the Hualapai Limestone Member. View west.

FIGURE 2.—Bedded oncolitic limestone of Hualapai Limestone Member in tributary on west side of Grapevine Canyon near locality 7 (fig. 1). Lake Mead and Grand Wash Cliffs can be seen in distance. View east.

sum of the Muddy Creek Formation. Above the gypsum is a 75-m sequence of well-bedded marl, limy claystone, and limy mudstone which is well exposed in steep ravines. Interfingering with this sequence are several layers of water-laid volcanic cinders and basalt cobbles. At about 36 m above the base of this sequence, a 150-mm bed of air-fall tuff (fig. 3) can be traced for more than 30 m. The volcanic glass shards in this bed have a K–Ar date of 8.66 ± 2.2 m.y. (Blair and others, 1977). Gypsum lenses up to 50 mm thick and 6 m long occur intermittently near the volcanic debris near the base of the Hualapai. Plant fossils are abundant (fig. 3). At places clumps and bundles of stems can be observed in positions of growth, and horizontal root structures weather out of the steep banks. The marl, claystone, and mudstone is overlain by 45 m of dense hard limestone which forms steep cliffs and resistant caps.

ROCK TYPES

The Hualapai Limestone Member consists of limestone interbedded with thin beds of limy claystone, mudstone, and siltstone. The weathered limestone beds of the Hualapai have a predominantly reddish color and form steep cliffs where they are dissected by Hualapai Wash. These cliffs are undercut in many places by erosion of the thin (5–15 cm) softer limy argillaceous interbeds. These argillaceous interbeds thicken and thin laterally over short distances.

Scattered chert nodules occur near the top of the Hualapai in a few places. Plant stems replaced by calcite and plant leaf impressions in the limestone are common locally. A few casts of small gastropods can be found in the dense limestone layers. Algal structures are abundant in some places. Thin lenses of impure gypsum beds as much as 50 mm thick are sparsely scattered throughout.

MINERALS

Chert nodules in some beds in the Hualapai Limestone Member in the western part of the study area (fig. 1, locs. 2 and 3) are weakly radioactive. The radioactive material consists of thin coatings of carnotite and autunite along bedding planes in the mudstone and claystone. These beds were staked as mineral claims in 1956. Preliminary reconnaissance reports from the Atomic Energy Commission (unpub. data) were submitted in 1955 and 1956 on these claims. The radioactive material ranged from 0.05 to 10.0 mR/hr on the Geiger counter. At the time of these reports, pockets of ore were considered too small and too widely scattered to be of commercial value. Some chert lenses were found to be radioactive. In several places bright yellow secondary uranium minerals can be seen surrounding the stems of opalized reed fossils. A few small chert lenses near a prospect pit in the top of the Hualapai in the vicinity of the type locality at Hualapai Wash are also weakly radioactive (fig. 1, loc. 6).

Chert nodules and thin beds of opal are much more common in the westernmost outcrop than at other exposures. Volcanic vents and flows that are associated with these outcrops probably supplied some silica to the waters in which the deposits were formed (Taliaferro, 1933), but no volcanic particulate material was seen in the siliceous rocks, so this source of silica is thought to be minor.

CHERT

The diagenetic sequences of siliceous rocks in the Hualapai Limestone Member are similar to opaline chert recovered from a wide variety of recent and ancient marine sedimentary deposits. We have examined samples of biogenic opal and cristobalite-rich rocks (called chert in this report) of the Hualapai Limestone Member under the scanning electron microscope (SEM) (pl. 5, figs. 2, 4, 6). This study reveals numerous free-growth forms of disordered cristobalite called lepispheres (Wise and Kelts, 1972, p. 188). These are microscopic spheres and hemispheres consisting of aggregates of cristobalite blades, usually 12–21 μm in diameter (pl. 4, figs. 1, 2; pl. 5, figs. 5, 6). The characteristic appearance of these minute lepispheres permits their identification by the SEM even when only one crystal cluster with a diameter of 2 μm is present (pl. 4, fig. 2).

X-ray diffraction patterns for siliceous material in the Hualapai Limestone Member (fig. 4*A*) are similar to those of marine rocks from opaline claystone of South Carolina (Wise and Weaver, 1973) (fig. 4*B*) and those from cores taken in the Antarctic Ocean (Wise and others, 1972) (fig. 4*C*). The X-ray patterns for siliceous material from the Hualapai are also similar to those produced by Calvert (1971) from deep-sea chert in the North Atlantic, those labeled "common opals" from Australia (Jones and others, 1964), and those from chert of the Monterey Shale of Miocene and Pliocene age (Ernst and Calvert, 1969).

The sedimentary rocks of the Muddy Creek Formation have been presumed to be derived from fresh to brackish waters (Longwell, 1928; Hunt, 1956; Lucchitta, 1972). However, the cristobalite-rich rocks of the Hualapai Limestone Member cannot be distinguished from marine rocks on the basis of SEM studies and X-ray analysis. Examples of marine siliceous rocks that resemble siliceous rocks of the Hualapai Limestone Member are: (1) opaline claystone of Eocene marine shallow shelf strata from Alabama to South

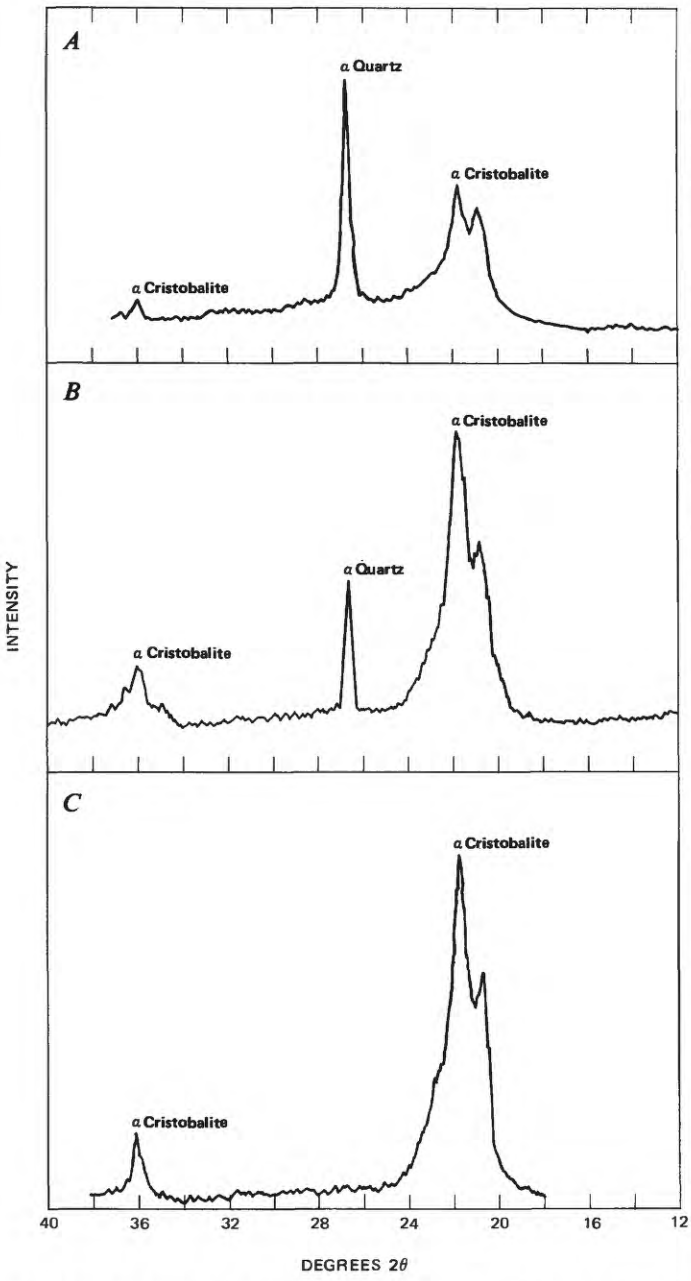

FIGURE 4.—X-ray diffraction patterns of marine rocks. *A*, Siliceous material from the Hualapai Limestone Member. *B*, Opaline claystone of South Carolina (Wise and Weaver, 1973). *C*, Core taken in the Antarctic Ocean (Wise and others, 1972).

Carolina (Wise and Weaver, 1973), (2) siliceous rocks of the Monterey Shale deposited in marginal Tertiary basins (Bramlette, 1946; Ingle, 1973; Murata and Larson, 1975; Murata and Nakata, 1974), and (3) deep-sea chert from the Antarctic, Pacific, and Atlantic Oceans (Berger and von Rad, 1972; Calvert, 1971; Heath and Moverly, 1971; Weaver and Wise, 1972a, b; Wise and Weaver, 1974).

Lepispheres in the opaline part of the Hualapai Limestone Member appear to be larger on the average but not as well formed as those seen in some marine chert (pl. 6, figs. 5, 6). At least one exception can be noted, however, in the micrographs of plate 3, figure 1. The larger lepisphere pictured here is very well rounded and symmetrical. A stereoscopic view shows that it is probably attached to the cavity walls by the small quartz crystals near its surface.

The scanning electron micrograph of plate 5, figure 4, shows clean cristobalite crystal blades with scalloped and serrated edges. Wise and Weaver (1973) noted cristobalite blades with similar serrated-edge patterns from marine opaline claystone of Alabama and from deep-sea chert.

Diatomaceous biogenic opal (opal-A of Jones and Segnit, 1971) is one of the most important sources of silica in pelagic sediment of recent oceans (Riedel, 1959). In fact, biogenic opal is the silica source for most deep-sea chert (Wise and others, 1972; Davies and Supko, 1973; Wise and Weaver, 1974). The evidence from the siliceous rocks in the Hualapai Limestone Member indicates that diatom frustules were the initial most important contributor to its nodular chert. This evidence reinforces the concept of the diagenetic sequence of biogenic opal (opal-A) to cristobalite (opal-CT) to chert. The authors subscribe to this kind of maturation sequence as advocated by Heath and Moberly (1971), Weaver and Wise (1972b), Berger and von Rad (1972), and Wise and Weaver (1974).

FOSSILS

ALGAL STROMATOLITES

The Hualapai Limestone Member contains circular to irregular oval objects from less than a millimeter to 10 cm in diameter (fig. 5). In thin section these show irregular banding (pl. 9, figs. 2, 4, 6; pl. 10, figs. 1–6, pl. 11, figs. 1–6, pl. 13, figs. 2–6; pl. 17, fig. 1; pl. 18, figs. 1–6). These we consider to be algal oncolites. Oncolites are unattached stromatolites with encapsulating laminae (Walter, 1976, p. 691). The specimens from the Hualapai Limestone Member (pl. 9, figs. 2, 4, 6; pl. 10, figs. 1–6) are similar in shape and size to Bradley's (1929, pls. 35, 42) digitated algae from the Green River Formation of Utah. Johnson (1961, pls. 132–133) shows similar specimens from the Green River Formation of Wyoming and Colorado.

Specimen 892D (pl. 9, figs. 2, 4, 6) of a digitate oncolite, is composed of irregular dark-brown and light bands of calcite which form botryoidal intergrowths. The narrower dark bands are composed of 3–5 μm calcite rhombs, whereas the lighter bands are formed by long slender calcite rhombs 50–100 μm long (pl. 9, fig.

FIGURE 5.—Outcrop of bedding surface covered with transverse section of algal oncolites, typical of much of the thick Hualapai Limestone Member. Photograph taken in first canyon north of Grapevine Canyon. Coin is 21 mm across.

6). Algal oncolites contain detrital quartz grains and fragments of volcanic rocks. The matrix that surrounds the algal oncolites is composed of detrital grains of quartz and volcanic rock in peloid-lime mudstone. These oncolites commonly have as their center or at their bases grains or pebbles of volcanic rocks or micritic mudlumps. Gebelein (1976) states:

> The environment of formation of oncolites at Joulters Cays, Bahamas, is similar to that for attached stromatolites, except that periodic turbulence, causing initial detachment of the forms, is higher. In the Joulters, this increase in turbulence corresponds to a decrease in depth. Maximum formation occurs in depths less than 1 m. Concentrations of 10–100 oncolites per m^2 are common in the shoal areas. Lags of oncolites carpet the floor of some tidal channels which cut through the shoals.

Algal oncolite specimen 846A (pl. 8, figs. 1–7) is a digitated form, with individual branches up to 1 mm in diameter. In transverse section the dark and light banding is somewhat circular, and in longitudinal section, the banding shows a distinct arched growth pattern. The long axes of the calcite crystals are tangential to the circular bands of the algae. Algal oncolites in transverse section, with crossed nicols, show a pseudo-uniaxial cross.

The algal oncolites from Grapevine Canyon (pl. 11, figs. 1–6) are up to 3 cm in diameter, are spherical in shape, and retain void spaces between oncolites. Voids within the oncolite and between growth bands are lined with cryptocrystalline quartz (opal) (pl. 11, figs. 5, 6).

Some algal oncolites (pl. 13, figs. 2, 4, 6) contain within their bands appreciable amounts of detrital quartz grains. Algal oncolites commonly are crusts on compound micrite mudlumps, formed of detrital quartz and micritic peloids (pl. 17, fig. 1). These algal crusts show a tendency for laminations developed on one side of the mudlump, suggesting growth upward (pl. 18, fig. 2).

Colloform algal stromatolites formed by digitate fabric occur in the Hualapai Limestone Member at Grapevine Canyon. Individual algal branches are 1–3 mm in diameter and may be up to 20–30 cm tall (pl. 8, figs. 1–6). Hoffman (1976) and Playford and Cockbain (1976) report colloform mat structures from the sublittoral shelf of Hamelin Pool, Shark Bay, Australia. These recent stromatolites have shapes similar to colloform stromatolites from the Hualapai Limestone Member. Hoffman's (1976, p. 269, figs. 6d, 6e) photographs of recent colloform tilted stromatolites are morphologically similar to the colloform stromatolites in the Hualapai. The Hamelin Pool colloform stromatolites live in a semiarid climate and subtidal

environment with salinity nearly twice that of normal seawater. Hoffman states that on the sublittoral floor, stromatolites with digitate columnar internal structure occur beneath ovoid patches of colloform mats. These colloform stromatolites are buried in pelleted lime mud. The Hamelin Pool fauna has low species diversity because of the hypersaline condition, and algae-consuming organisms are largely absent (Playford and Cockbain, 1976). As a result algal stromatolites flourish on the sublittoral and intertidal platforms. In Hamelin Pool lithification of stromatolites has taken place in both the intertidal and subtidal environments. Laminations are only crudely developed or absent in many Hamelin Pool stromatolites, and fenestrate (birdseye) fabrics are characteristic.

Shinn (1968) recognized two kinds of birdseye structures in recent and ancient carbonate rocks: (1) planar isolated vugs 1–3 mm high by several millimeters wide and (2) isolated bubblelike vugs 1–3 mm in diameter. Both types are generally filled with calcite or anhydrite.

Shinn's study of more than 100 cores and samples of recent carbonate sediments showed that birdseye voids are preserved in supratidal sediments (sediments deposited above normal high-tide level), sometimes in intertidal sediments (sediments deposited between normal and high-tide level), sometimes in intertidal sediments (sediments deposited between normal high and normal low tide), and never in subtidal sediments (sediments permanently below water). Both kinds of birdseyes are particularly abundant in supratidal dolomitic sediments.

Playford and Cockbain's (1976, p. 410, fig. 11A) example of a well-lithified intertidal stromatolite from Hamelin Pool, showing the characteristic fenestral fabric in weakly laminated pellet wackestone, is similar to fenestrate pellet packstone of the Hualapai Limestone Member (pl. 10, figs. 1–6; pl. 13, figs. 1, 3, 5; pl. 15, figs. 1, 6).

DIATOMS

Diatoms were recovered by J. Platt Bradbury, of the U.S. Geological Survey, from opalized rock samples we collected near the top of the Hualapai Limestone Member at localities 1 and 4 (fig. 1). He identified the specimens from locality 1 as *Scoliopleura* sp., *Nitzchia* sp., *Mastogloia* cf. *M. aquilegiae, Rhopalodia gibberula, Navicula* cf. *N. radiosa tenella, Amphora* or *Cymbella* sp., and *Denticula* sp.

White opal from an outcrop of the Hualapai Limestone Member 6 km southeast of Temple Bar (fig. 1, loc. 4) was studied by the authors under the scanning electron microscope. This study revealed the existence of exceptionally well preserved diatoms imbedded in the opal. Scanning electron micrographs of these diatoms are presented on plate 1. Bradbury has identified these species (written commun., 1976) as *Navicula* cf. *N. cuspidata* (pl. 1, fig. 1) which is widespread in alkaline freshwater habitats. *Navicula halophila* (pl. 1, fig. 2) is a true brackish-water diatom that can tolerate considerable variations in salinity. This diatom is characteristic of inland lakes and marshes of moderate salinity but it is also found in coastal (marine) environments.

Melosira moniliformis? (pl. 1. figs. 5, 6), *Amphora hyalina* (pl. 1, fig. 4), and *Amphora arcus* var. *sulcata* (pl. 1, fig. 3) are marine or brackish-water diatoms that are common in coastal littoral habitats. Frequently *Amphora* species occur in estuarine environments.

According to Bradbury, *Melosira moniliformis?, Amphora arcus* var. *sulcata,* and *Amphora hyalina* seldom characterize inland saline aquatic environments. Their presence suggests that a coastal, perhaps estuarine, environment existed when the diatomaceous sediments were deposited.

The diatoms suggest that the Hualapai Limestone Member is not older than Neogene. The diatom family *Epithemiaceae* which includes the genera *Denticula* and *Rhopalodia* is thought not to be older than Pliocene.

PLANT FOSSILS

The remains of grasses, reeds, and rushes are the most abundant macrofossils found in the Hualapai Limestone Member. These can be observed as layered horizontal mats entirely replaced by limestone. Others form vertical hollow calcite tubes, having inner surfaces lined with drusy quartz and exteriors encrusted with travertine. In at least one locality (fig. 1, loc. 1) the reed stem structures have been perfectly replaced by opal, preserving the cell walls (pl. 12, figs. 1–6). Molds and casts of the plants resemble *Juncus* (*Juncaceae,* the rush family), but they have not been identified with certainty.

Some of the plant fossils with hollow stem structures look like scouring rushes (*Equisetacae*): these rushes are now represented only by a single genus, *Equisetum* (Robinson and Fernald, 1908, p. 51; Scott, 1962, p. 13). The stems usually have hollow internodes with a coating of silex, which is the zone that is normally preserved. *Equisetum* is a silica accumulator plant that takes silica into its system from the soil. This silica is precipitated around the cell walls in the form of plant opal (Lovering and Engel, 1967, p. B15). When the plant dies, the silica then is either dispersed in the form of phytoliths, or, if the plant is buried before this dispersal, its opalized structure can be preserved in the

rock record. The amount of silica contributed to the Hualapai Limestone Member in this manner, however, was probably minor.

GASTROPODS

Gastropod molds and steinkerns were collected at several localities in the Hualapai Limestone Member and were studied by J. H. Hanley (unpub. data). One poorly preserved complete steinkern of a sinistral gastropod may represent the Physidae. This specimen was one of several collected by the authors from Hualapai Wash (fig. 1, loc. 5). Twenty incomplete external molds and four incomplete steinkerns collected from locality 4 (fig. 1) may represent a single species of *Flumnicola* Stimpson. *Flumnicola* is known from two other localities in the Muddy Creek Formation in Clark County, Nev.: (1) USGS Cenozoic locality 22250, Dry Lake quadrangle. E½ sec. 35, and W½ sec. 36, T. 19 S., R. 63 E., carbonate facies. Collected by C. R. Longwell, 1960, and (2) USGS Cenozoic locality 22252 (L10–58). SW½ sec. 26, T. 19 S., R. 63 E., calcareous facies. Collected by W. H. Hays, 1958.

The *Hydrobiidae,* which includes *Flumnicola,* are herbivorous, ingesting algae and algal detritus, but diatoms constitute the principal food source for some species. Hydrobiids occur in aquatic habitats of many sizes, from creeks and springs to the Great Lakes. Some species occur in brackish and marine habitats. These gastropods live on a variety of substrates including mud, sand, gravel, and aquatic plants.

The wide-ranging habitats of the fossil gastropods of the Hualapai Limestone Member preclude their use as indicators of the paleoenvironment.

OSTRACODES

Ostracodes are locally abundant in the Hualapai Limestone Member. Several ostracodes were observed in thin section. None could be definitely classified, but at least one individual resembles a species of *Candona* (J. P. Bradbury, written commun., 1976). *Candona* is typical of the freshwater forms, which are characterized by smooth and monotonous surface features (Benson, 1961). Species of *Candona* are found in all types of freshwater environments, ranging from deep water to marshes. They are nonswimmers, usually burrowing in the mud. Over 100 species of *Candona* have been described (Van Morkhoven, 1963). Its eggs not only require no care but can stand desiccation for long periods of time. On the other hand, the eggs of marine ostracodes cannot survive any drying out whatsoever (Kesling, 1961).

Ostracode remains from limestone near Grapevine Canyon appear relatively abundant under the scanning electron microscope (pl. 6, figs. 1, 3), and in thin section (pl. 17, fig. 4). These were too poorly preserved to be classified, but they also resemble *Candona.*

Opaline rocks containing reed fossils from an area 12 km southwest of Temple Bar (fig. 1, loc. 1) were etched for 24 hours in a solution of one part hydrofluoric acid to nine parts of water. Many silicified ostracode valves were freed from the matrix, but these were also poorly preserved (pl. 6, figs. 1, 3).

TRACE FOSSILS

Distinctive flask-shaped casts about 2 cm in diameter occur in the Hualapai Limestone Member 12 km southwest of Temple Bar marina. These distinctive fossils weather out from clayey limestone beds in the side of a road cut.

These casts invariably have much the same shape and dimensions. They are alined perpendicular to the bedding planes of the sediments within a few centimeters of each other, probably much in the same position as they were formed in life. They are calcareous thin-walled tubular structures, broken at the upper end and closed in a bulbous form at the lower end. The open end tapers inward slightly to form a neck, which then enlarges downward to produce the ovoid base.

Jerome G. Rozen, Jr., of the American Museum of Natural History, has suggested (written commun., 1976) that these fossils are cells of aculeate Hymenoptera (bees and wasps). Probably these casts are remains of nests of a large, solitary, ground-nesting bee. That is, they are chambers into which the female bee carried pollen and nectar and in which she laid her eggs. The narrow rounded ends of the cell in these chambers seem to be unusual and remind Rozen of a bee of the southwest, *Ptiloglossa,* which he has studied. This genus belongs to a primitive family of bees which could easily have been here 8.5 m.y. ago.

Nest patterns of solitary bees vary from species to species and genus to genus. They usually consist of a burrow descending into the ground with branching passages and with cells at the ends of the branches (fig. 6).

CARBONATE ROCKS

Dunham's (1962) carbonate rock classification is used in this report. The Hualapai Limestone Member, as studied in the stratigraphic section near Grapevine Canyon (fig. 2), is composed predominantly of micritic limestone. The only significant fossil bioclasts here are algal oncolites, rare fragments of ostracodes, and mollusks. The limestone is porous, owing to incomplete sparry calcite cementation between micrite mudlumps, algal oncolites, and pellets.

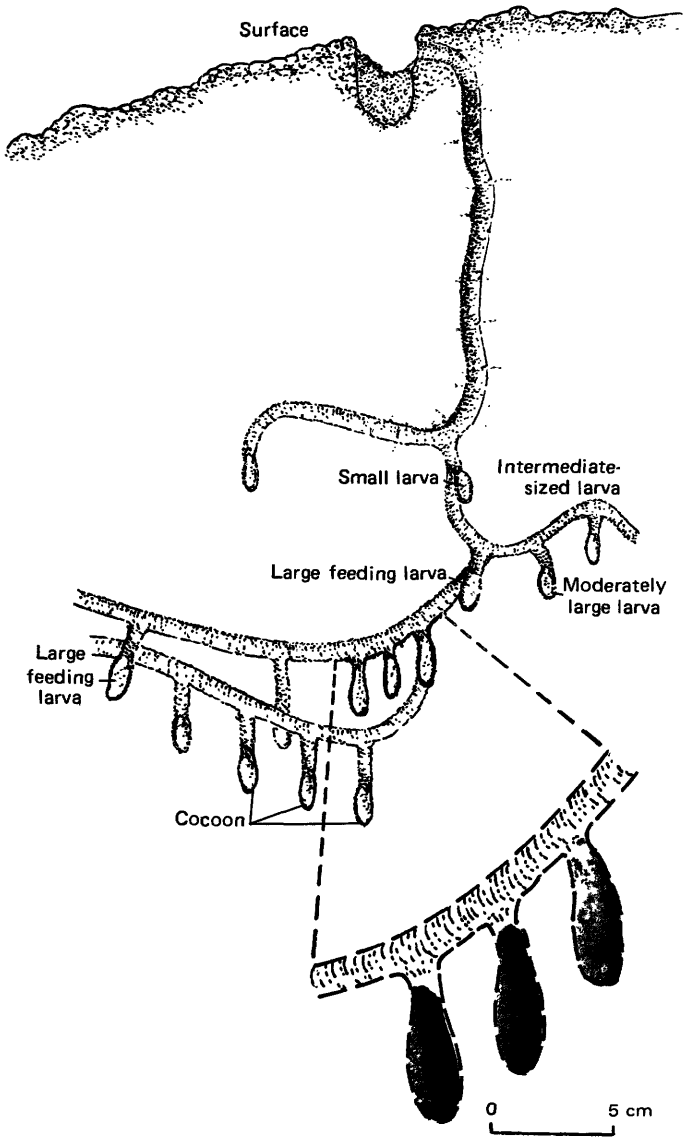

FIGURE 6.—Nest of a large, solitary, ground-nesting bee with photographs of fossil casts for comparison. Modified from Rozen (1974).

Terrigenous admixtures are abundant in the micritic carbonate rocks of the Hualapai Limestone Member. They are silt- and sand-size quartz grains and fragments of volcanic rocks (pl. 9, fig. 2; pl. 10, fig. 1; pl. 12, figs. 4–6; pl. 13, figs. 2, 4, 5; pl. 16, figs. 2–6; pl. 18, figs. 1, 2; pl. 19, figs. 1, 2, 4).

DIAGENESIS

For the purpose of this paper, diagenesis will include all changes that sediments undergo from the time of deposition until the present (Wood and Armstrong, 1975, p. 15). One of these changes is lithification, the change from unconsolidated sediment to consolidated sediment by compaction, cementation, and pressure solution.

MATRIX

Matrix is usually composed of carbonate mud (micrite) and is dominantly of biologic origin. The separation of grains and matrix is to some extent a function of the scale of observation, but in practice a tendency toward a bimodal size distribution in micritic limestone makes the distinction easy. Individual crystals of micrite have an upper size limit of 3–4 μm (Bathurst, 1959). Choquette and Pray (1970, p. 247) define interparticulate porosity for between-particle porosity in sedimentary carbonates. It can be used for lime mud and micrites as well as for coarser clastic carbonate.

Recent carbonate mud is largely bioclastic in origin, whether originally aragonite (described by Cloud, 1962) or calcitic in composition (Davies, 1970). The only known examples of inorganic precipitation of calcium carbonate are in the lagoon of Abu Dhabi (Kinsman and Holland, 1969) and Trucial Cast, Persian Gulf (Evamy, 1973), and the lower to middle intertidal zone of Shark Bay, Australia (Logan, 1974). Stockman, Ginsburg, and Shinn (1967) have shown that great quantities of aragonite mud can be produced by codiacean algae in Florida Bay and can more than account for the aragonite mud present.

The abundant micrite (pls. 14–18) in the Hualapai Limestone Member is probably the result of organic activity by codiacean and other algae. The absence of fossil bioclasts, other than algal oncolites and a rare ostracode, precludes significant formation of micrite derived from larger shelled invertebrates.

SPARRY CALCITE

Primary pore space and interparticle space are still present within the Hualapai Limestone Member. Two distinct phases of sparry calcite cement are found within the interparticle space. The first-phase cement forms a thin fringe of relatively constant thickness of 40 μm around the algal oncolites and peloids (Shinn, 1969) (pl. 10, figs. 2, 3, 5; pl. 13, figs. 1, 5, 6; pl. 18, fig. 6). These are stubby calcite crystals with pyramidal terminations growing at right angles to the grain margins. Bathurst (1971, p. 432) shows that the first generation of cement crystals, besides being smaller, are commonly scalenohedral in habit (dogtooth spar) and are preserved under the later overgrowth of second-generation rhombohedra. The sharp distinction in size and habit between the earlier and later crystals may indicate a time interval between formation of the two sizes.

The source of the calcium carbonate necessary for the complete cementation implies that the second-phase cement is from another source. Bathurst (1971, p. 457) suggested that neither solution of local aragonite nor pressure solution will provide sufficient volume to nearly obliterate the intergranular space. Within the Hualapai Limestone Member a very large proportion of the originally aragonitic micrite and bioclasts has gone into solution by vadose waters and has been redeposited as void-filling sparry calcite. This process could provide the large amount of sparry calcite cement seen in the Hualapai (pl. 10, figs. 1–6; pl. 13, figs. 1–6; pl. 15, figs. 1–6; pl. 16, figs. 1–4; pl. 17, fig. 4; pl. 18, figs 1–6).

RADIAXIAL FIBROUS CALCITE

Limestone specimens from the section south of Grapevine Canyon have numerous cavities filled with fibrous radiaxial calcite (pl. 15, figs. 4, 5; pl. 16, figs. 4, 5; pl. 19, figs. 1–6). The radiaxial cement occurs as void-filling material between algal oncolites, in lime mudlumps, and in fenestrate voids in the lime mudstone. The radiaxial fibrous calcite typically contains numerous zones of inclusions (fig. 7) The inclusion zones may be parallel to the substrate. The most common type of inclusion is scalenohedral forms that may reveal the positions of former calcite crystal faces (pl. 18, fig. 1).

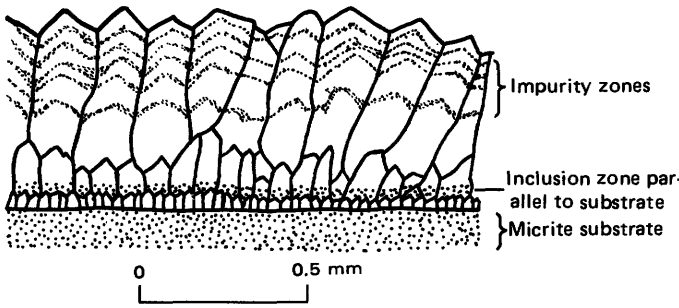

FIGURE 7.—Radiaxial fibrous calcite cement and inclusion patterns in the Hualapai Limestone Member. Greater part of mosaic is composed of fibrous crystals, long axes oriented normal to substrate. Marginal zones exhibit decrease in crystal size toward substrate.

Kendall and Tucker (1973) in the detailed discussion of the origin and environmental significance of radiaxial fibrous calcite indicate that it is a replacement after acicular cement. They state, "* * *acicular cement appears to be largely restricted to marine, early diagenetic environments. Consequently, formation of radiaxial fibrous mosaics also occurs during early diagenesis."

AGE

An air-fall tuff 15 cm thick, that is completely within the lower part of the Hualapai Limestone Member, crops out at locality 1 (fig. 1) 12 km southwest of Temple Bar. The glass shards of this tuff have yielded a K-Ar date of about 8.7 ± 2.2 m.y. (Blair and others, 1977; see table 1), considered to be late Miocene.

The maximum and minimum age limits of the Hualapai Limestone Member are not known. However, a basalt in the lower part of the exposed section of the Muddy Creek Formation 6 km southeast of Temple Bar (fig. 1, loc. 4) underlies the Hualapai. This basalt has been dated using the K-Ar method by McKee (unpub. data; see table 1) at about 10.9 m.y.

A basalt flow at Sandy Point (fig. 1) separated from the underlying Muddy Creek Formation by fluvial gravel has been dated at 3.79 ± 0.46 m.y. by Damon (Damon and others, 1978, p. 102).

DISCUSSION AND CONCLUSIONS

The Hualapai Limestone Member, considered by most workers to be freshwater in origin, has many similarities to marine deposits (Blair, 1978). The water which deposited the Hualapai was most likely con-

TABLE 1.—*K-Ar analytical data and ages of samples*

[Analysis by E. H. McKee, U.S. Geological Survey]

Locality	Sample	K_2O (percent)	$^{40}Ar^{rad}$ (mole/g)	$^{40}Ar^{rad}$ (percent)	Age[1] (m.y.)	Age[2] (m.y.)	Source
(fig. 1, loc. 1)	Basaltic shards in air-fall tuff, lower part of Hualapai Limestone Member	2.462	3.07633×10^{-11}	7.1	$8.44 + 2.23$	8.66 ± 2.2	Blair and others, (1977).
(fig. 1, loc. 4)	Basalt below Hualapai Limestone Member	1.045 1.067	1.66192×10^{-11}	17.1	10.62 ± 1.10	10.90 ± 1.1	E. H. McKee (unpub. data).

[1]Ages based on old constants for comparison with published ages.
$\lambda\epsilon = 0.58 \times 10^{-10}yr^{-1}$
$\lambda\beta = 4.72 \times 10^{-10}yr^{-1}$
cp4 5-10yr-1
$^{40}K/K_{total} = 1.22 \times 10^{-4}g/g$

[2]Ages based on new constants.
$\lambda\epsilon = 0.581 \times 10^{-10}yr^{-1}$
$\lambda\beta = 5.96 \times 10^{-10}yr^{-1}$
$^{40}K/K_{total} = 1.17 \times 10^{-4}g/g$

nected with the upper reaches of the Gulf of California in late Miocene time and was hence the upper estuarine part of the ancestral gulf. Marine beds of the Pliocene Bouse Formation (Metzger, 1968), which were deposited in the ancestral Gulf of California, have been mapped as far north as the Parker area, about 180 km south of the southernmost exposures of the Hualapai Limestone Member (fig. 8). This embayment no doubt reached further north. This arm of the ancestral Gulf of California (Karig and Jensky, 1972) probably extended to the foot of the Grand Wash Cliffs as a shallow estuary.

Marine, brackish, and freshwater fossil assemblages occur together in the Bouse Formation, a phenomenon that puzzled Smith (1970) when she studied the fossils of that formation. She speculated, however, that such

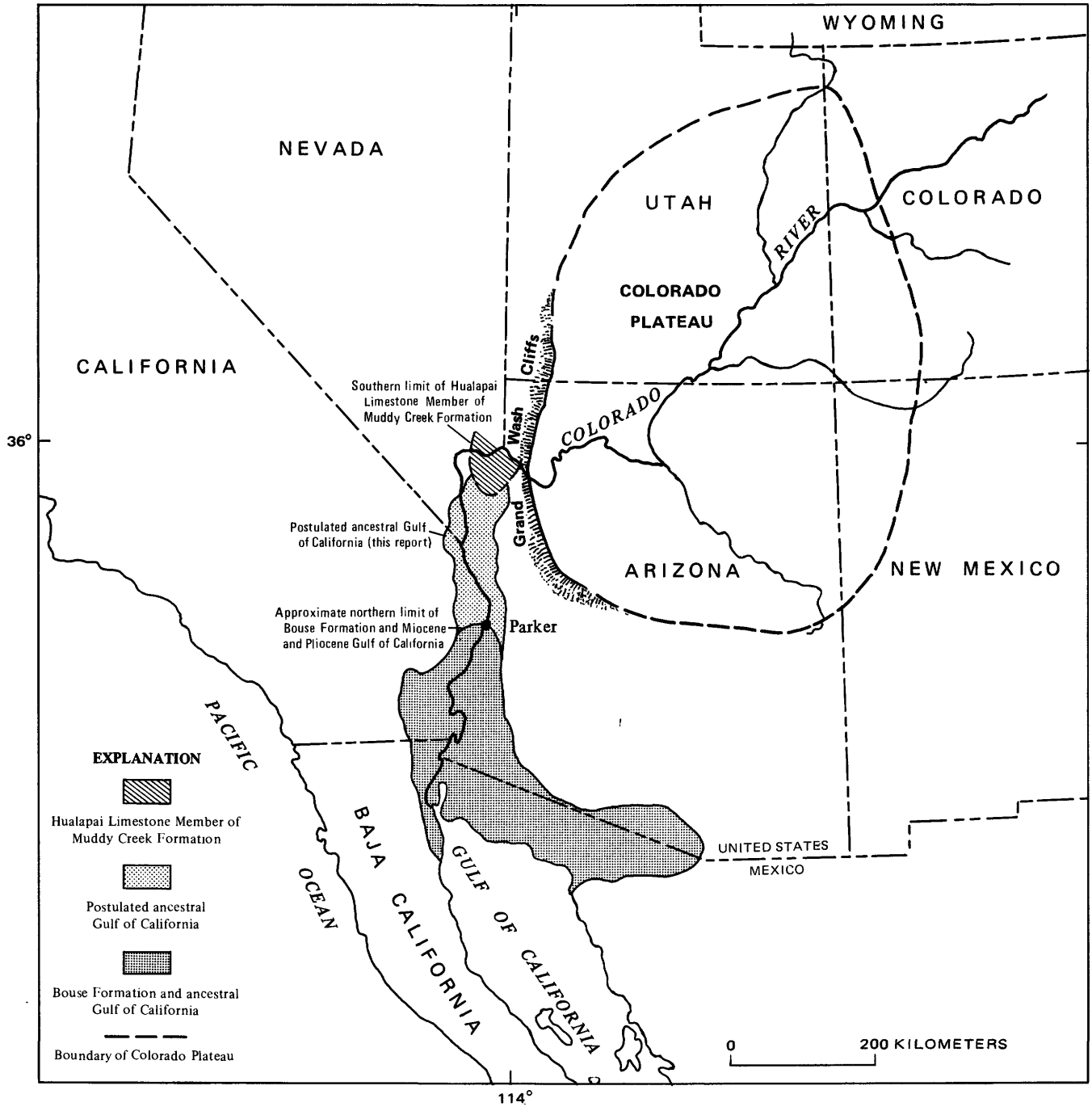

FIGURE 8.—Miocene and Pliocene embayment of Gulf of California. Modified from Schuchert, (1955); Metzger, (1968); and Smith, (1970).

an assemblage might be due to mixing of fossils by sedimentary processes. The restricted number of species of foraminifers found in the northern areas of the Bouse is typical of modern bays and estuaries. Freshwater mollusks and ostracodes are found with the foraminifers, but the presence of marine clams and snails classifies the Bouse Formation as marine.

Several lines of evidence indicate that as the Hualapai Limestone Member was being deposited, seawater was mixing with fresh water in an estuary:

(1) Marine coastal and estuarine diatoms occur together with freshwater forms in the upper part of the Hualapai Limestone Member (pl. 1, figs. 1–6).

(2) Freshwater and marine fossil assemblages are mixed in the Hualapai, as in the Bouse Formation to the south. A logical source for the freshwater types would be from a river (the ancestral Colorado River) entering from the north.

(3) Existing data suggest that the diagenesis of biogenic opal conversion to chert occurs predominantly in marine environments. However, Oehler (1973) experimentally produced lepispheres in water with only about 700 ppm of Na^+; this concentration approaches fresh water. This study may show that lepispheres can also form an estuarine environment.

(4) The mass of limestone (over 100 km^3) indicates a large volume of water containing calcium, probably seawater.

(5) Radiaxial fibrous calcite cement fills voids between algal oncolites and micritic lithoclasts in the Hualapai Limestone Member. Radiaxial fibrous calcite cement is considered to be largely restricted to marine environments.

(6) Stromatolites from the Hualapai Limestone Member are typical of forms found in shallow marine environments (fig. 6).

(7) An air-fall tuff in the lower part of the Hualapai was dated at about 8.7 m.y. (table 1).

The hypothesis that would account for all this data is that a shallow, marshy, marine estuary existed in late Miocene time, extending up the area of the lower Colorado River to the base of the Colorado Plateau where the river now emerges from the Grand Canyon. The elevation at this point was then at sea level, some 420 m lower than it is now. A large slow-moving river (the ancestral Colorado River?) entered the estuary from some unknown direction.

REFERENCES CITED

Bathurst, R. G. C., 1959, Diagenesis in Mississippian calcilutites and pseudobreccias: Jour. Sed. Petrology, v. 29, p. 365–376.

———1971, Carbonate sediments and their diagenesis: Amsterdam, Elsevier, 620 p.

Benson, R. H., 1961, Ecology of ostracode assemblages, *in* Moore, R. C., ed., Treatise on invertebrate paleontology, Pt. Q, Arthropoda 3: Lawrence, Kans., Geol. Soc. American and Kansas Univ. Press, p. Q56–Q63.

Berger, W. H., and Rad, Ulrich von, 1972, Cretaceous and Cenozoic sediments from the Atlantic Ocean, *in* Hayes, D. E., and others, eds., Initial reports of the Deep Sea Drilling Project; Lisbon, Portugal to San Juan, Puerto Rico: Deep Sea Drilling Proj. Initial Rept. v. 14, p. 788–954.

Blacet, P. M., 1975, Preliminary geologic map of the Garnet Mountain quadrangle, Mojave County, Arizona: U.S. Geol. Survey Open-File Rept. 75–93, scale 1:48,000.

Blair, W. N., 1978, Gulf of California in Lake Mead area of Arizona and Nevada during Late Miocene time: Am. Assoc. Petroleum Geologists Bull., v. 62, no. 7, p. 1159–1170.

Blair, W. N., McKee, E. H., and Armstrong, A. K., 1977, Age and environment of deposition of the Hualapai Limestone member of the Muddy Creek Formation [abs.]: Geol. Soc. America Abs. with Programs, v. 9, no. 4, p. 390–391.

Bradley, W. H., 1929, Algae reefs and oolites of the Green River Formation: U.S. Geol. Survey Prof. Paper 154–G, p. G203–G223.

Bramlette, M. N., 1946, The Monterey Formation of California and the origin of its siliceous rocks: U.S. Geol. Survey Prof. Paper 212, 57 p.

Calvert, S. E., 1971, Nature of silica phases in deep sea cherts of the North Atlantic: Nature, v. 234, no. 50, p. 133–134.

Choquette, P. W., and Pray, L. C., 1970, Geologic nomenclature and classification of porosity in sedimentary carbonates: Am. Assoc. Petroleum Geologists Bull., v. 54, no. 4, p. 207–250.

Cloud, P. E., Jr., 1962, Environment of calcium carbonate deposition west of Andros Island, Bahamas: U.S. Geol. Survey Prof. Paper 350, p. 1–138.

Damon, P. E., Shafiqullah, M., and Scarborough, R. B., 1978, Revised chronology for critical stages in the evolution of the lower Colorado River: Geol. Soc. America Cordilleran Sec., Abs. with Programs, v. 10, no. 3, p. 101–102.

Davies, G. R., 1970, Carbonate bank sedimentation, Eastern Shark Bay, Western Australia, *in* Carbonate sedimentation and environment, Shark Bay, Western Australia: Am. Assoc. Petroleum Geologists Mem. 13, p. 85–168.

Davies, T. A., and Supko, P. R., 1973, Oceanic sediments and their diagenesis; Some examples from deep drilling: Jour. Sed. Petrology, v. 43, p. 381–390.

Dunham, R. J., 1962, Classification of carbonate rocks according to depositional textures, *in* Hams, W. E., ed., Classification of carbonate rocks: Am. Assoc. Petroleum Geologists Mem. 7, p. 108–121.

Ernst, W. G., and Calvert, S. E., 1969, An experimental study of the recrystallization of porcelanite and its bearing on the origin of some bedded cherts: Am. Jour. Sci, v. 267–A, p. 114–133.

Evamy, B. D., 1973, The precipitation of aragonite and its alteration to calcite on the Trucial Coast of the Persian Gulf, *in* Purser, B. H., ed., The Persian Gulf: New York, Springer-Verlag, p. 329–431.

Gebelein, C. D., 1976, Open marine subtidal and intertidal stromatolites, *in* Walters, M. R., ed. Developments in sedimentology 20, Stromatolites: Amsterdam, Elsevier, p. 261–271.

Heath, G. R., and Moberly, R., 1971, Cherts from the western Pacific, Leg 7, *in* Winterer, E. L., and others, eds., Initial reports of the Deep Sea Drilling Project: Deep Sea Drilling Proj. Initial Rept., v. 7, p. 991–1007.

Hoffman, P., 1976, Stromatolite morphogenesis in Shark Bay, Western Australia, *in* Walter, M. R., ed., Developments in sedimentology 20, Stromatolites: Amsterdam, Elsevier, p. 261–271.

Hunt, C. B., 1956, Cenzoic geology of the Colorado plateau: U.S. Geol. Survey Prof. Paper 279, 99 p.

Ingle, J. C., 1973, Pliocene-Miocene sedimentary environments and biofacies, southeastern Los Angeles Basin-San Joaquin Hills area, Orange County, California, *in* Miocene sedimentary environment and biofacies, southeastern Los Angeles Bay: Am. Assoc. Petroleum Geologists, Soc. Econ. Paleontologists and Mineralogists, and Soc. Econ. Geologists Ann. Mtg., 1973, SEPM Trip 1 Guidebook, pl. 1–6.

Johnson, J. H., 1961, Limestone building algae and algal limestones: Golden, Colo., Colorado School Mines, 297 p.

Jones, J. B., Sanders, J. V., and Segnit, E. R., 1964, Structure of opal: Nature, v. 204, p. 990–991.

Jones, J. B., and Segnit, E. R., 1971, The nature of opal. I. Nomenclature and constituent phases: Geol. Soc. Australia Jour., v. 18, p. 56–68.

Karig, D. E., and Jensky, W., 1972, The proto-Gulf of California: Earth and Planetary Sci. Letters 17, p. 169–174.

Kendall, A. C., and Tucker, M. E., 1973, Radiaxial fibrous calcite—A replacement after acicular carbonate: Sedimentology, v. 20, p. 365–389.

Kesling, R. V., 1961, Reproduction of ostracoda, *in* Moore, R. C., ed., Treatise on invertebrate paleontology, pt. Q, Arthropoda 3: Lawrence, Kans., Geol. Soc. America and Kansas Univ. Press, P. A17–A19.

Kinsman, D. J. J., and Holland, H. D., 1969, The co-precipitation of cations with $CaCO_3$. The co-precipitation of Sr^{2+} with aragonite between 16° and 96°C: Geochim. et Cosmochim. Acta, v. 33, p. 1–17.

Logan, B. W., 1974, Inventory of diagenesis in Holocene—Recent carbonate sediments, Shark Bay, Western Australia, *in* Evolution and diagenesis of Quaternary carbonate sequences, Shark Bay, Western Australia: Am. Assoc. Petroleum Geologists Mem. 22, p. 195–247.

Longwell, C. R., 1928, Geology of the Muddy Mountains, Nevada: U.S. Geol. Survey Bull. 798, 152 p.

———1936, Geology of the Boulder Reservoir floor, Arizona: Geol. Soc. America Bull., v. 47, p. 1393–1476.

———1954, Geologic setting of Lake Mead, *in* Smith, W. O., and others, Lake Mead comprehensive survey of 1948–49, Volume I: U.S. Dept. Interior and U.S. Dept. Navy coop. project, p. 1116–1128.

Longwell, C. R., Pampeyan, E. H., Bowyer, Ben, and Roberts, R. J., 1965, Geology and mineral deposits of Clark County, Nevada: Nevada Bur. Mines Bull. 62, 218 p.

Lovering, T. S., and Engel, Celest, 1967, Translocation of silica and other elements from rock into *Equisetum* and three grasses: U.S. Geol. Survey Prof. Paper 594–B, 16 p.

Lucchitta, Ivo, 1967, Cenozoic geology of the upper Lake Mead area adjacent to the Grand Wash Cliffs, Arizona: University Park, Penn., Pennsylvania State Univ., Ph.D. thesis, 218 p.

———1972, Early history of the Colorado River in the Basin and Range province: Geol. Soc. America Bull., v. 83, no. 7, p. 1933–1947.

Metzger, D. G., 1968, The Bouse Formation (Pliocene) of the Parker-Blythe-Cibola area, Arizona and California, *in* Geological Survey research 1968: U.S. Geol. Survey Prof. Paper 600–D, p. D126–D136.

Murata, K. J., and Larson, R. R., 1975, Diagenesis of Miocene siliceous shales, Temblor Range, California: U.S. Geol. Survey Jour. Research, v. 3, no. 5, p. 553–566.

Murata, K. J., and Nakata, J. K., 1974, Cristobalitic stage in the diagenesis of diatomaceous shale: Science, v. 184, p. 567–568.

Oehler, J. H., 1973, Tridymite-like crystals in cristobalitic "cherts": Nature, Phys. Sci., v. 241, no. 107, p. 64–65.

Playford, P. E., and Cockbain, A. E., 1976, Modern algal stromatolites at Hamelin Pool, a hypersaline barred basin in Shark Bay, Western Australia, *in* Walters, M. R., ed., Developments in sedimentology 20, Stromatolites: Amsterdam, Elsevier, p. 389–411.

Peirce, H. W., 1976, Tectonic significance of Basin and Range thick evaporite deposits: Arizona Geol. Soc. Digest, v. 10, p. 325–339.

Riedel, W. R., 1959, Siliceous organic remains in the pelagic sediments: Soc. Econ. Paleontologists and Mineralogists Spec. Pub. 7, p. 80–91.

Robinson, B. L., and Fernald, M. L., 1908, Grey's new manual of botany, a handbook of the flowering plants and ferns of the central and northeastern United States and Canada: New York, America Book Co., 926 p.

Rozen, J. G., Jr., 1974, Nest biology of the Eucerine bee *Thygater analis* (Hymenoptera, Anthoporidae): Jour. New York Entomol. Soc., v. 82, no. 4, p. 230–234.

Schuchert, Charles, 1955, Atlas of paleogeographic maps of North America: New York, John Wiley & Sons, 177 p.

Scott, D. H., 1962, Studies in fossil botany (3d ed.): New York, Hafner, v. 1, 434 p.

Shinn, E. A., 1968, Practical significance of birdseye structures in carbonate rocks: Jour. Sed. Petrology, v. 38, no. 1, p. 221–224.

———1969, Submarine lithification of Holocene carbonate sediments in the Persian Gulf: Sedimentology, v. 12, p. 109–144.

Smith, P. B., 1970, New evidence for Pliocene marine embayment along the lower Colorado River area, California and Arizona: Geol. Soc. America Bull., v. 81, p. 1411–1420.

Stock, Chester, 1921, Late Cenozoic mammalian remains from the Meadow Valley region, southeastern Nevada [abs.]: Geol. Soc. America Bull., v. 32, p. 146–147.

Stockman, K. W., Ginsburg, R. N., and Shinn, E. A., 1967, The production of lime mud by algae in south Florida: Jour. Sed. Petrology, v. 37, p. 633–648.

Taliaferro, N. L., 1933, The relation of volcanism to diatomaceous and associated siliceous sediments: California Univ. Pubs. Geol. Sci., v. 23, no. 1, 56 p.

Van Morkhoven, F. P. C. M., 1963, Post-Paleozoic ostracoda: Amsterdam, Elsevier, v. 2, 478 p.

Walter, M. R., 1976, Glossary of selected terms, Appendix I *of* Walter, M. R., ed., Developments in sedimentology 20, Stromatolites: Amsterdam, Elsevier, p. 687–692.

Weaver, F. M., and Wise, S. W., 1972a, Chertification phenomena in Antarctic and Pacific deep sea sediments—A scanning electron microscope and X-ray diffraction study: Am. Assoc. Petroleum Geologists Bull. 56, p. 1905.

———1972b, Ultramorphology of deep sea cristobalitic chert: Nature Phys. Sci., v. 237, p. 56–57.

Wise, S. W., Buie, B. F., and Weaver, F. M., 1972, Chemically precipitated sedimentary cristobalite and the origin of chert: Eclogae Geol. Helvetiae, v. 65/1, p. 157–163.

Wise, S. W., and Kelts, K. M., 1972, Inferred diagenetic history of a weakly silicified deep sea chalk: Gulf Coast Assoc. Geol. Soc. Trans., v. 22, p. 177–203.

Wise, S. W., and Weaver, F. M., 1973, Origin of cristobalite-rich Tertiary sediments in the Atlantic and Gulf Coastal Plain: Gulf Coast Assoc. Geol. Soc. Trans., v. 23, p. 305–323.

——1974, Chertification of oceanic sediments: Internat. Assoc. Sedimentology Spec. Pub. 1, p. 301–326.

Wood, G. V., and Armstrong, A. K., 1975, Diagenesis and stratigraphy of the Lisburne Group limestones of the Sadlerochit Mountains and adjacent areas, northeastern Alaska: U.S. Geol. Survey Prof. Paper 857, 47 p.

PLATES 1–19

Contact photographs of the plates in this report are available, at cost, from U.S. Geological Survey Library, Federal Center, Denver, Colorado 80225

PLATE 1

FIGURES 1–6. Scanning electron micrographs of diatoms found together in opaline rock in the Hualapai Limestone Member. The diatoms range in habitat from freshwater to marine. All are from locality 4 (text fig. 1).

1. *Navicula* cf. *N. cuspidata*.
   Diatom widespread in freshwater habitats.
2. *Navicula halophila*.
   This is a true brackish-water diatom.
3. *Amphora arcus* v. *sulcata*.
   Marine or brackish-water diatom.
4. *Amphora hyalina*.
   Marine or brackish-water diatom.
5. *Melosira moniliformis?*
   Interior view. Marine or brackish-water diatom.
6. *Melosira moniliformis?*

1 0 10μm

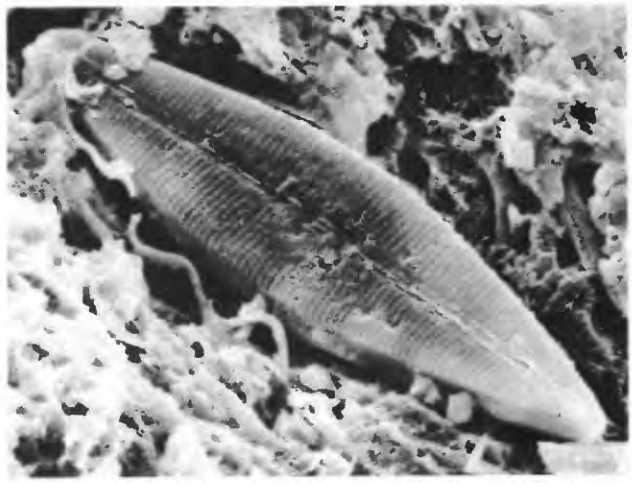

2 0 10μm

3 0 10μm

4 0 6μm

5 0 30μm

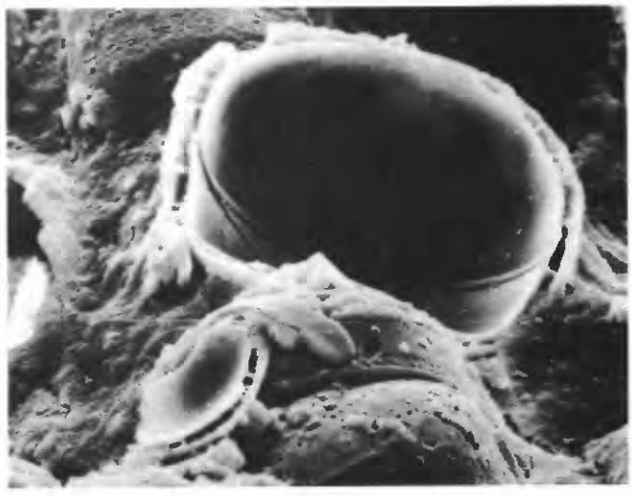

6 0 30μm

DIATOMS

PLATE 2

FIGURES 1–6. Scanning electron micrographs showing progressive conversion of biogenic silica to cristobalite-rich chert.

1. Slightly altered diatom frustules.
2. Diatom frustules filled with bladed cristobalite.
3. Diatom frustule partly filled with bladed cristobalite. Remainder is filled with chert.
4. Altered diatoms which are gradually losing their identities.
5. Vestiges of diatom frustules merging in chert.
6. Cristobalite chert with textures and fossil evidence obliterated.

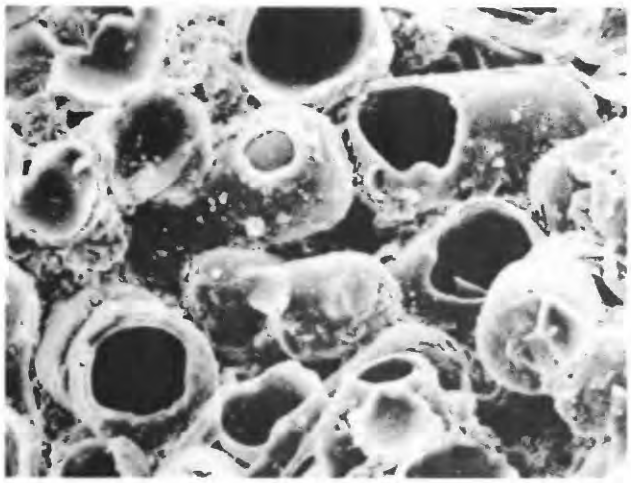

1 0 60μm

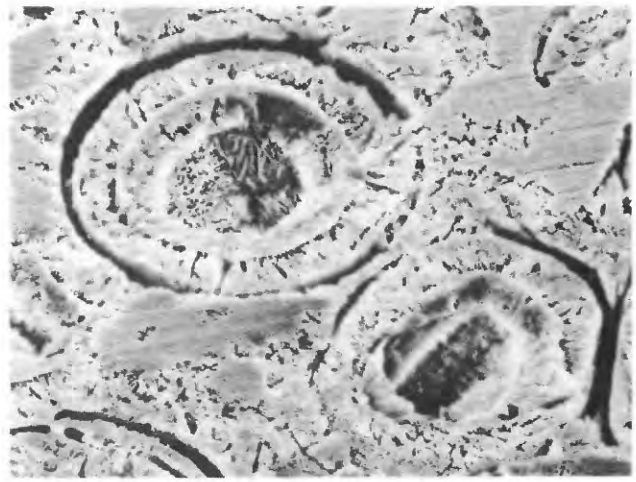

2 0 30μm

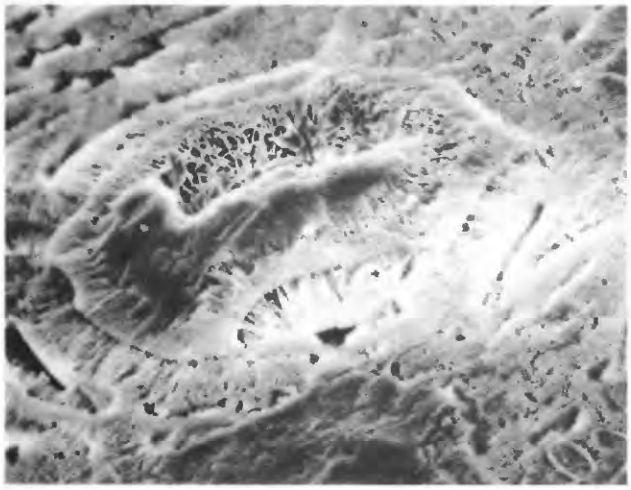

3 0 10μm

4 0 30μm

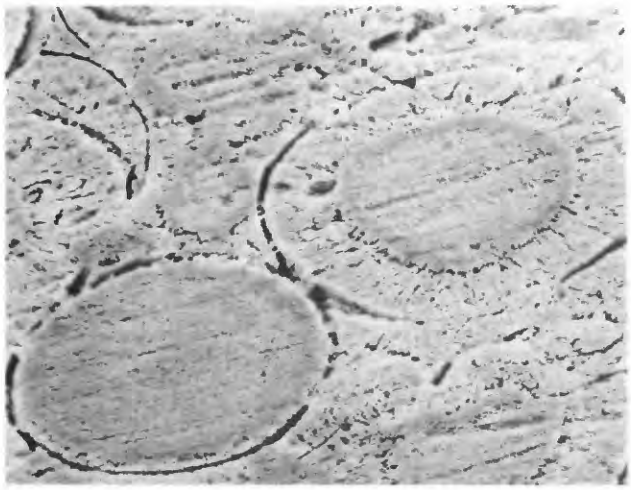

5 0 30μm

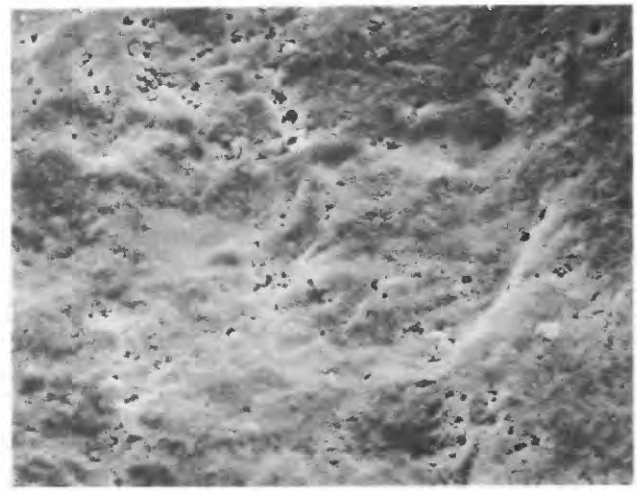

6 0 20μm

CONVERSION OF BIOGENIC SILICA TO CRISTOBALITE-RICH CHERT

PLATE 3

FIGURES 1, 2. Scanning electron micrographs showing lepispheres of bladed cristobalite in chert sample from locality 4 (text fig. 1).

1. Stereopair set at 65 mm interocular distance. Well-formed lepisphere was growing in cavity in chert. Small embryonic lepispheres are scattered about cavity. Note small quartz crystal penetrating sphere at its upper right quadrant.
2. Enlargement of embryonic lepispheres indicated by arrow in figure 1.

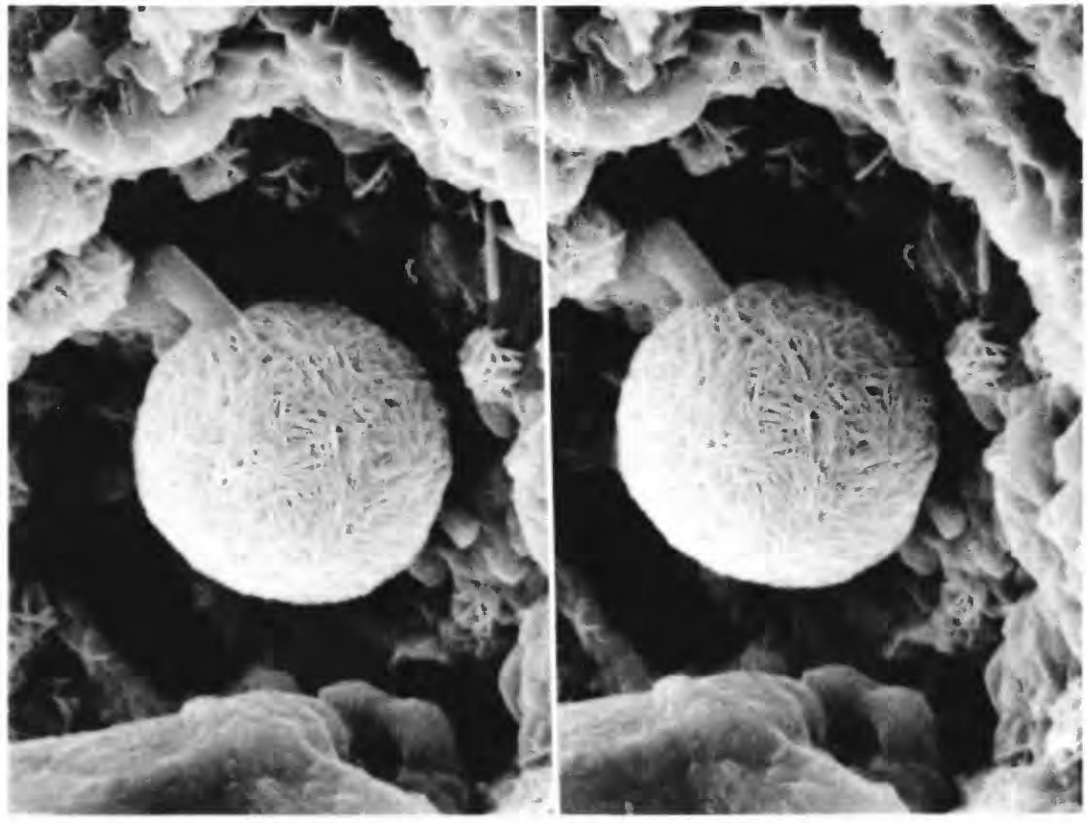

1 0 6μm

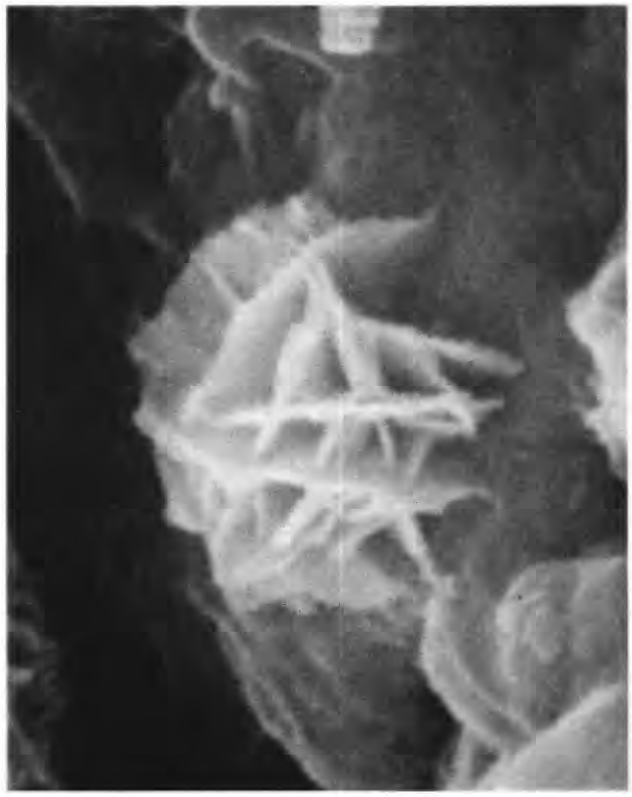

2 0 1μm

LEPISPHERES OF BLADED CRISTOBALITE

PLATE 4

FIGURES 1–6. Scanning electron micrographs and elemental distribution maps of opaline and chert samples from locality 2 (text fig. 1).

1. Slightly altered diatom frustules.
2. Silicon distribution map of figure 1.
3. Feathery cristobalite crystals lining vug in plant fossil (pl. 7, fig. 1).
4. Silicon distribution map of figure 3.
5. Diatom mold filled with cristobalite crystal blades.
6. Silicon distribution map of figure 5.

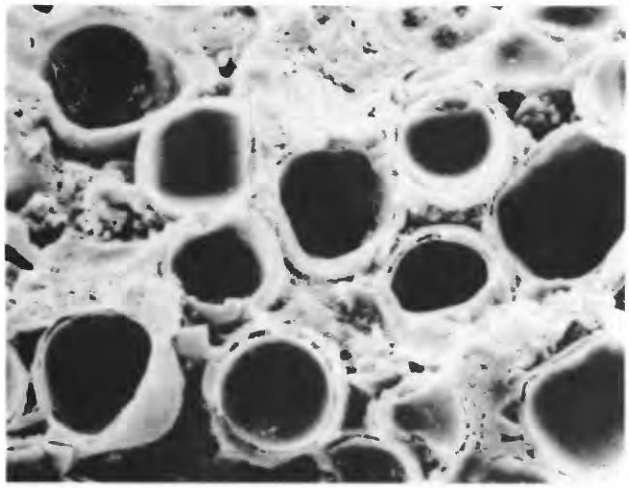

1

0 30μm

2

3

0 10μm

4

5

0 10μm

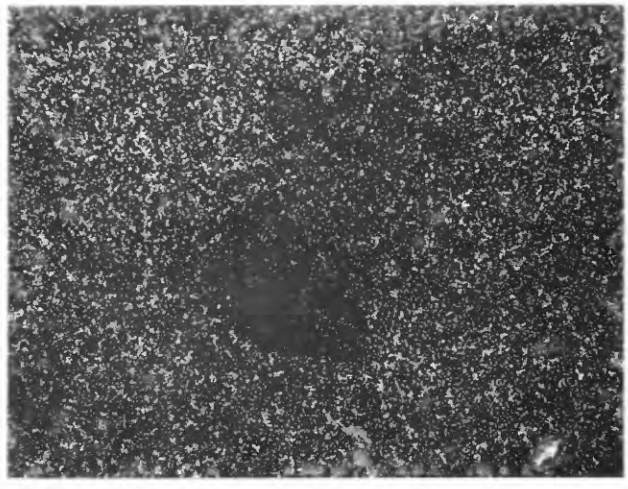

6

OPALINE AND CHERT SAMPLES

PLATE 5

FIGURES 1–6. Scanning electron micrographs of opaline material. Figures 1–4 from locality 4 (text fig. 1). Figures 5, 6 from locality 2 (text fig. 1).

1. Altered diatom frustule embedded in chert.
2. Diatom frustule similar to that shown in figure 1 but with part of its outer shell gone. Well-developed cristobalite crystals line interior of mold.
3. Diatom frustule exposed after grinding surface of opaline sample.
4. Enlargement of cristobalite crystals in figure 2. Note scalloped and serrated edges of crystal blades.
5. Irregular-shaped lepispheres growing in vug in chert.
6. Symmetrical lepispheres in opaline cavity.

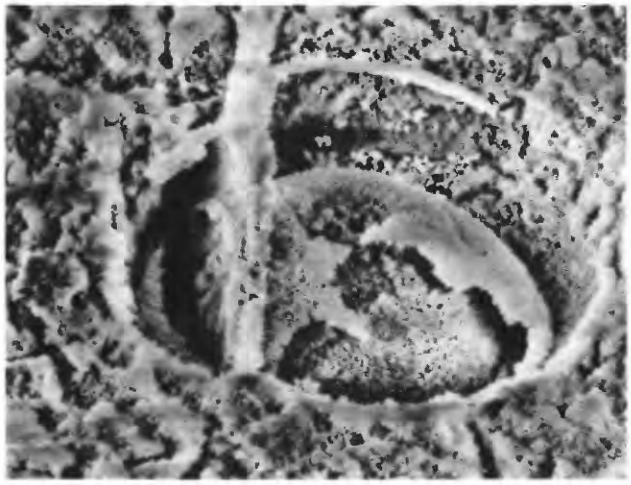

1 0 10μm

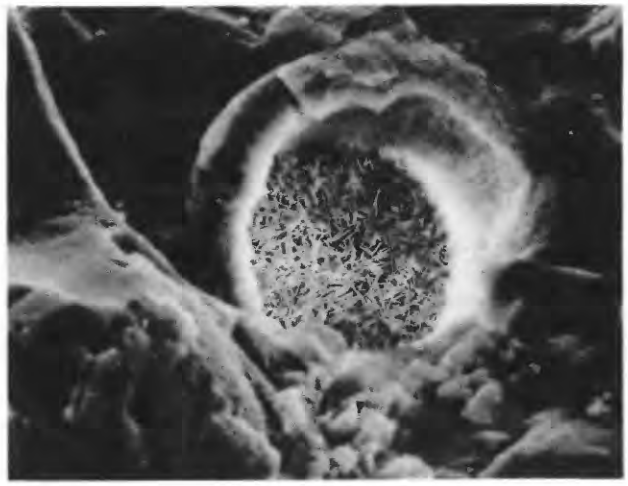

2 0 10μm

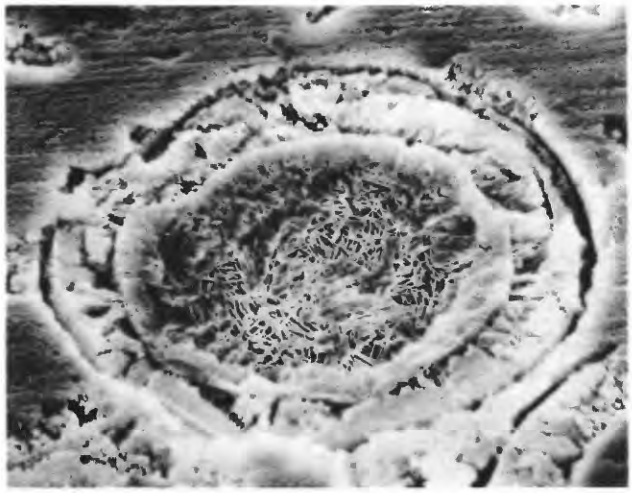

3 0 10μm

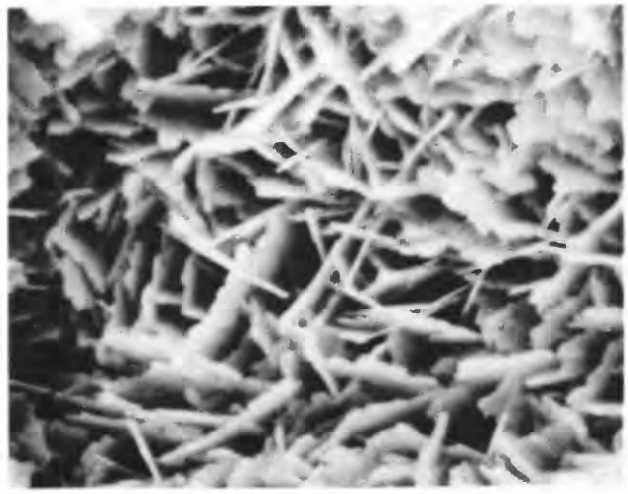

4 0 3μm

5 0 10μm

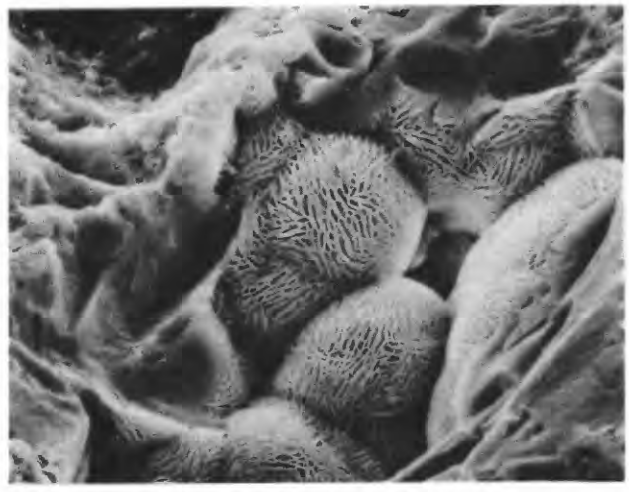

6 0 20μm

OPALINE MATERIAL

PLATE 6

FIGURES 1–6. Scanning electron micrographs of ostracode valves and seed etched from siliceous matrix using 10 percent hydrofluoric acid. Samples from locality 2 (text fig. 1).

1. Single ostracode valve replaced by silica.
2. Enlargement of figure 1 showing surface features.
3. Two ostracode valves replaced by silica.
4. Enlargement of figure 3 showing surface features.
5. Unidentified fossil seed replaced by calcite.
6. Enlargement of figure 5 showing surface composed of calcite crystals.

1 0 100μm

2 0 6μm

3 0 100μm

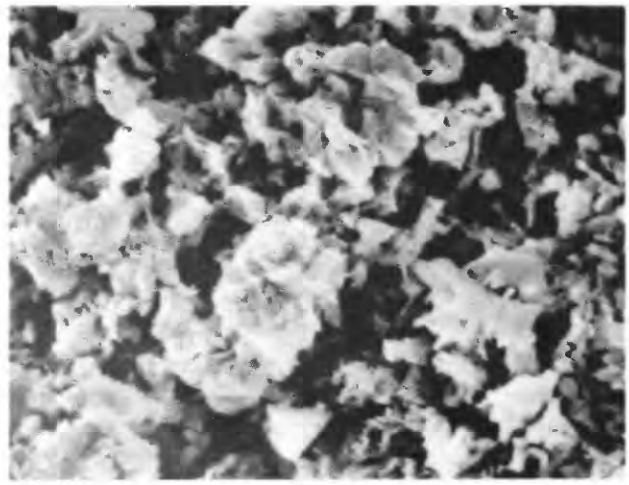

4 0 6μm

5 0 100μm

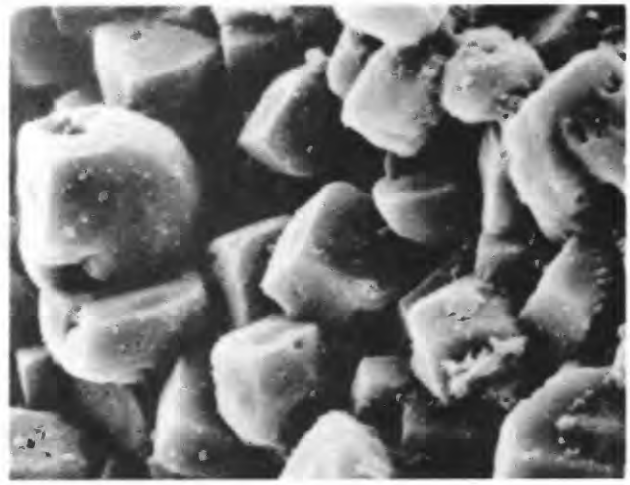

6 0 6μm

OSTRACODE VALVES ETCHED FROM SILICEOUS MATRIX

PLATE 7

FIGURES 1–6. Scanning electron micrographs of fossil plants in the Hualapai Limestone Member. Samples from locality 1 (text fig. 1).

1. Transverse section of fossil reed showing interior filling of chalcedony.
2. Enlargement of reed filling in figure 1.
3. Fossil plant molds in limestone.
4. Enlargement of surface of fossil shown in left side of figure 3.
5. Chalcedony filling of cavity between reed fossils in limestone.
6. Chalcedony filling cavity between fossil plants in limestone.

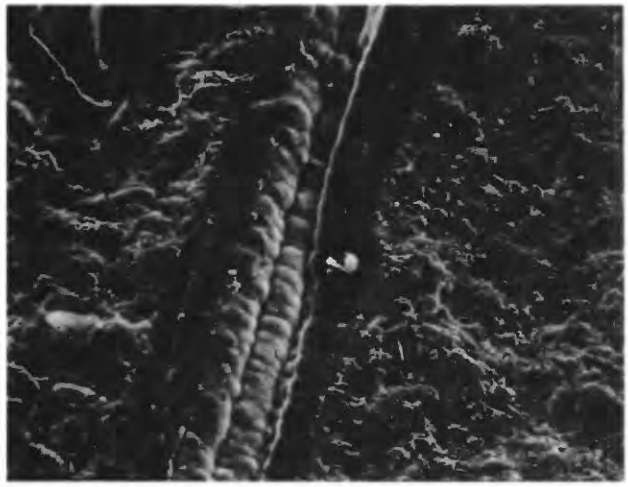

1 0 60μm

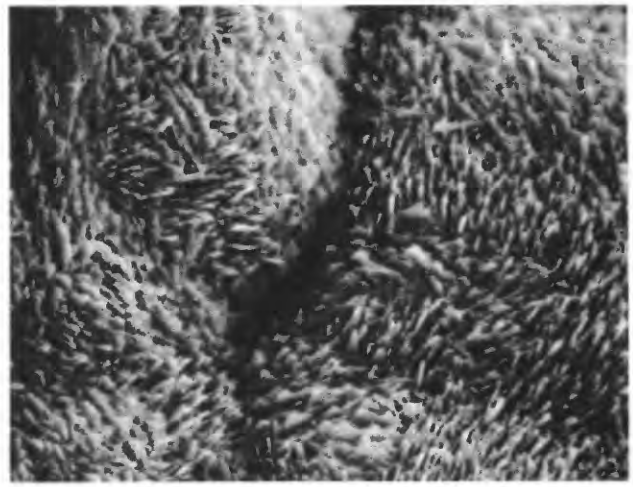

2 0 3μm

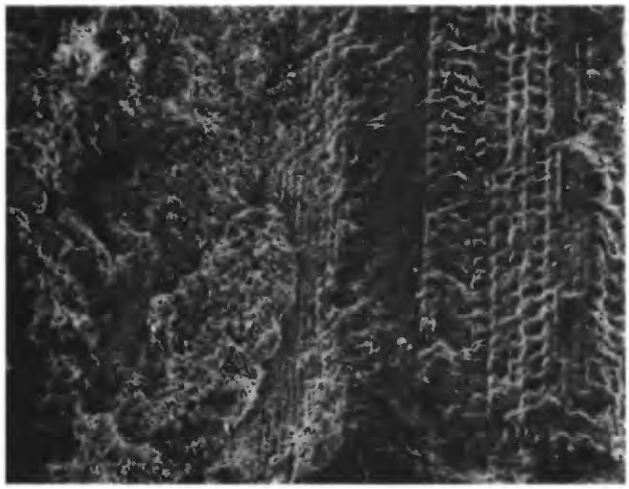

3 0 100μm

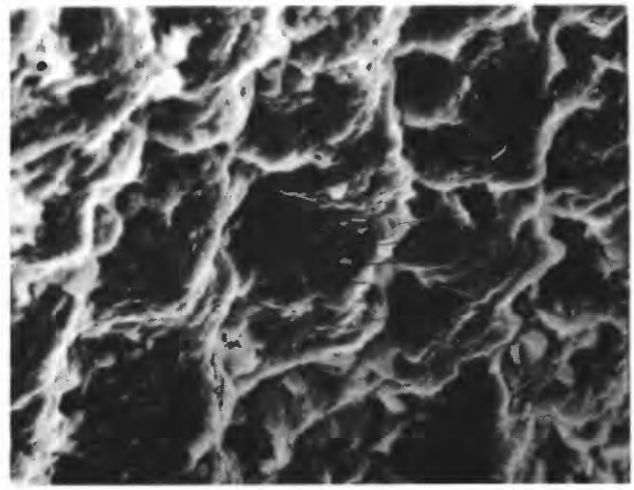

4 0 10μm

5 0 30μm

6 0 100μm

FOSSIL PLANTS

PLATE 8

FIGURES 1–7. Algal limestone; Hualapai Limestone Member, Grapevine Canyon. Specimen 846A.

1, 2. Longitudinal and transverse view of nearly parallel branches of calcareous algae.

3, 4. Transverse view of calcareous algae branch showing radial banding. 3, White areas shown by arrow are detrital quartz fragments. Circular bands are composed of radiaxial calcite. Light bands are composed of fibrous calcite up to 0.2–0.3 mm long. Narrower dark bands are formed by subhedral calcite crystals 20 to 50 mm in size and possibly iron-rich inclusions.

5, 6. Longitudinal view, showing arched dark and light banding of algal branches. Figure 6 shows in detail fibrous calcite that forms bands.

7. Scanning electron micrograph of calcareous algae. Calcite rhombs range in size from 3 to 15 m. Siliceous, microcrystalline silica (S) and clay (cy) minerals stand in relief.

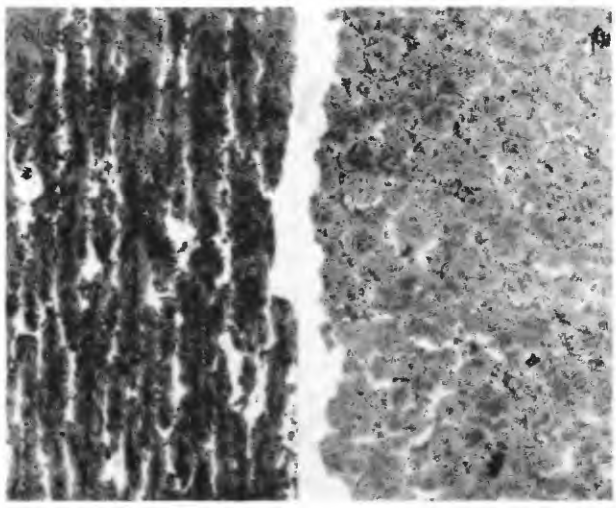

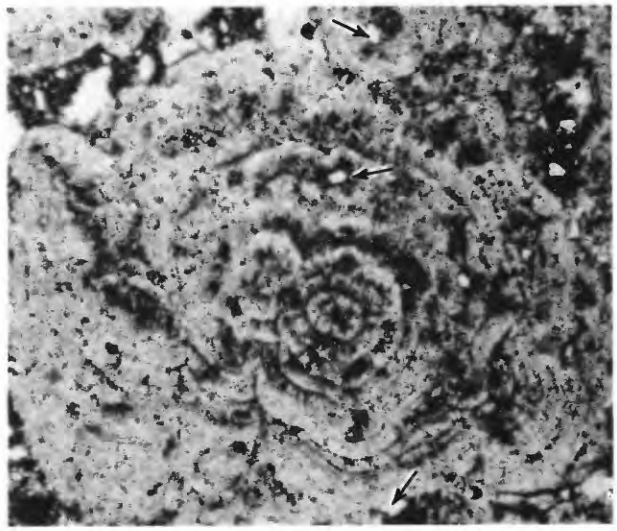

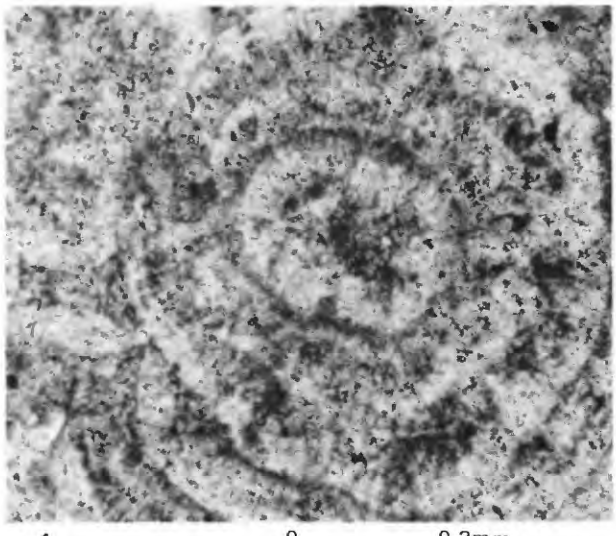

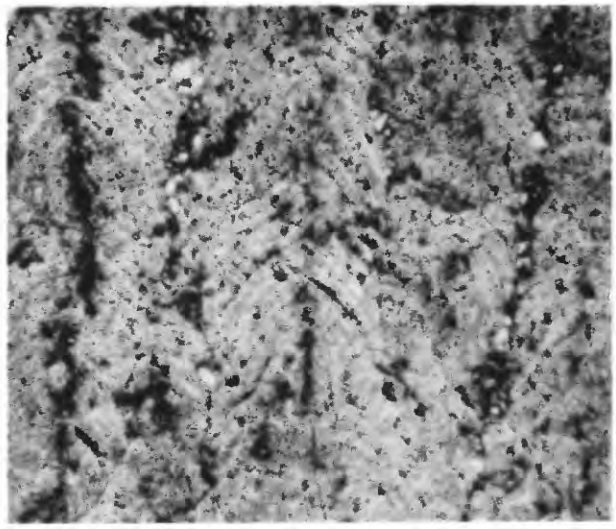

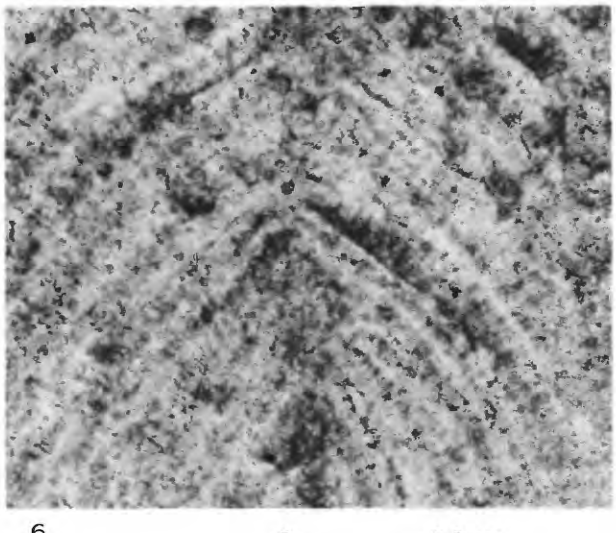

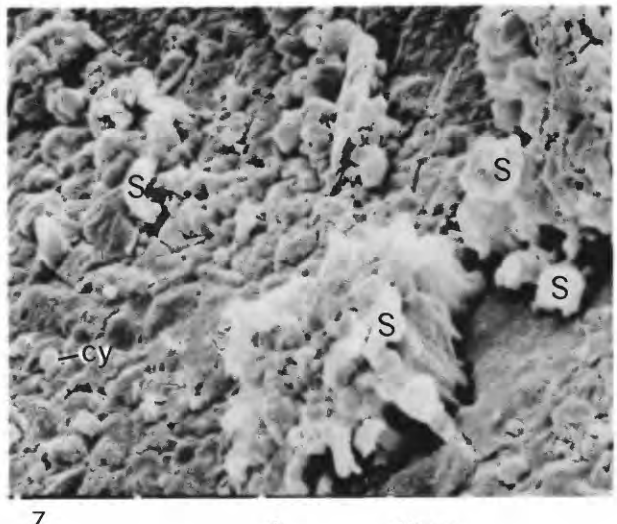

ALGAL LIMESTONE

PLATE 9

FIGURES 1–6. Pisolites and microstructures, Hualapai Limestone Member.

1, 3, 5. Pisolite structures formed by radiaxial fibrous calcite (cr); dark bands formed by iron oxide-rich zones. 3, Pisolitic structures formed by radiaxial fibrous calcite (cr); dark area in upper half of view formed of microcrystalline chalcedony (ch). 5, Details of light bands of radiaxial calcite (cr) and dark narrow bands of iron oxide-rich calcite (D). Specimen 876B.

2, 4, 6. 2, Rock is formed of volcanic fragments (vf), dark areas, silt- and sand-size grains of angular quartz, and algal nodules and branches (A). 4, 6, Enlarged view of structure illustrating wide light bands and narrow dark bands. Specimen 892D.

1

0 0.5mm

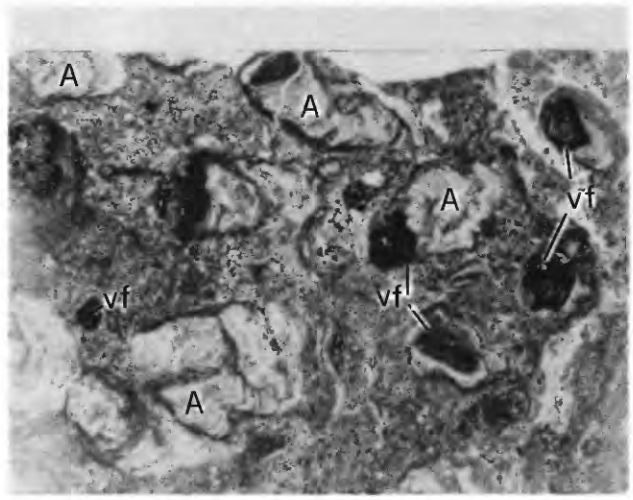

2

0 10mm

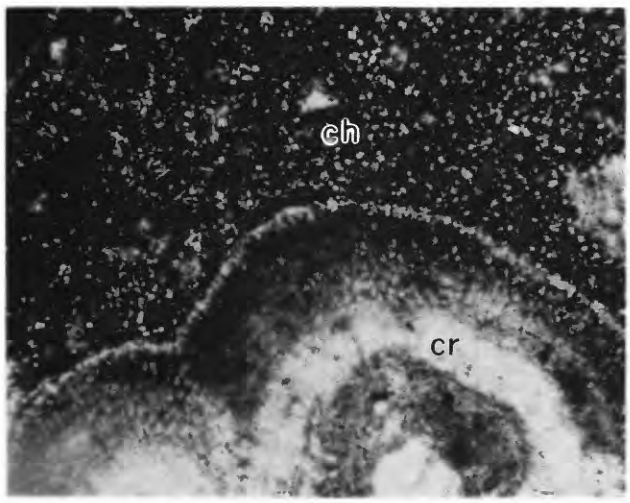

3

0 0.5mm

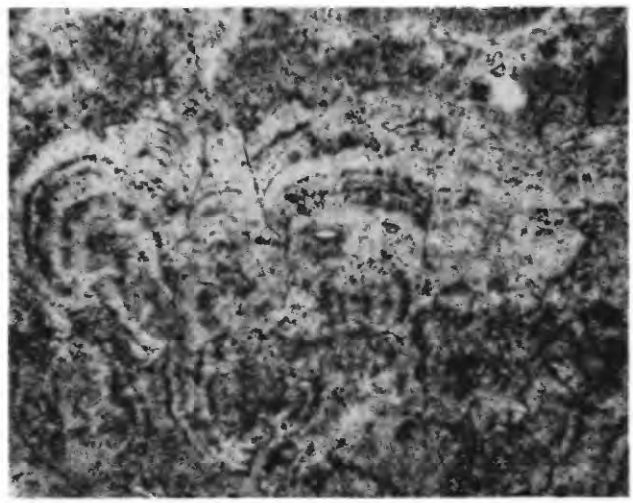

4

0 1mm

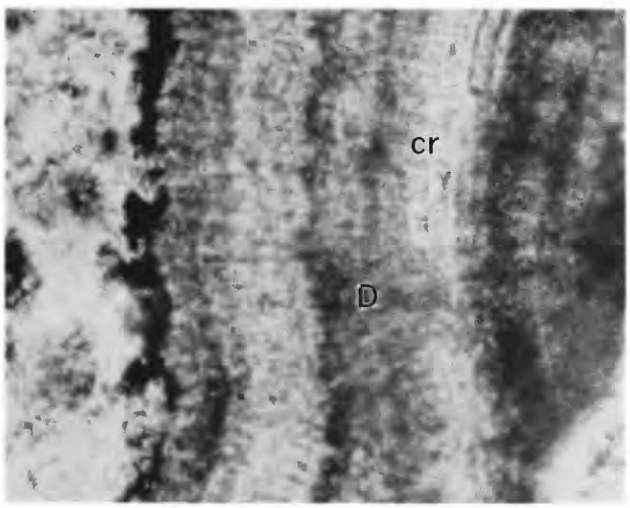

5

0 0.2mm

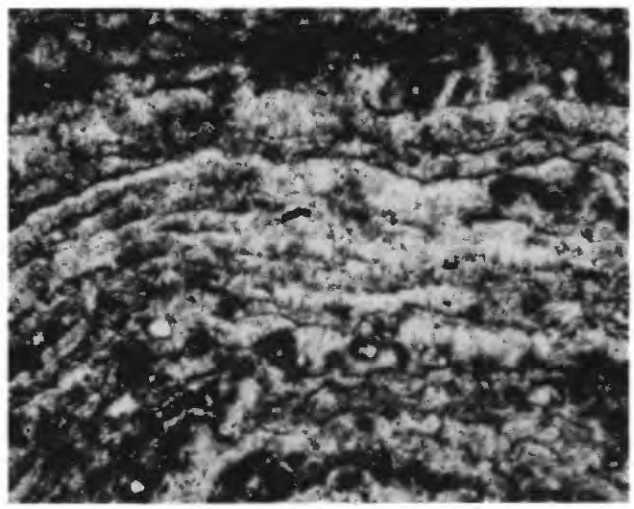

6

0 0.5mm

PISOLITES AND MICROSTRUCTURES

PLATE 10

FIGURES 1–6. Fenestrate peloid packstone, Hualapai Limestone Member.

1. Pellets are from 50 to 100 μm in size, have poorly defined outlines, and are composed of calcite crystals 2–4 μm in size. Subrounded quartz grains are up to 0.3 mm in size.
2. Details of peloids, showing surface of peloids covered by early-stage, first-phase calcite cement that is stubby calcite crystals with pyramidal terminations growing at right angles to grain margins (cp); voids between peloids were then filled by sparry calcite (cs). Specimen 800A.

3, 4. Peloid packstone; rock is free of quartz sand grains. 3, Outlines of peloids are poorly defined; peloids are typically 50–100 μm in diameter. 4, Peloids are composed of calcite crystals 3–6 μm in size. Areas between peloids are filled by sparry calcite cement (cs). Specimen 800B.

5, 6. Peloid packstone. Peloids are formed by 4–8-μm calcite crystals. Outlines of individual peloids are poorly defined. Area between peloids is filled by sparry calcite (cs). Specimen 800C.

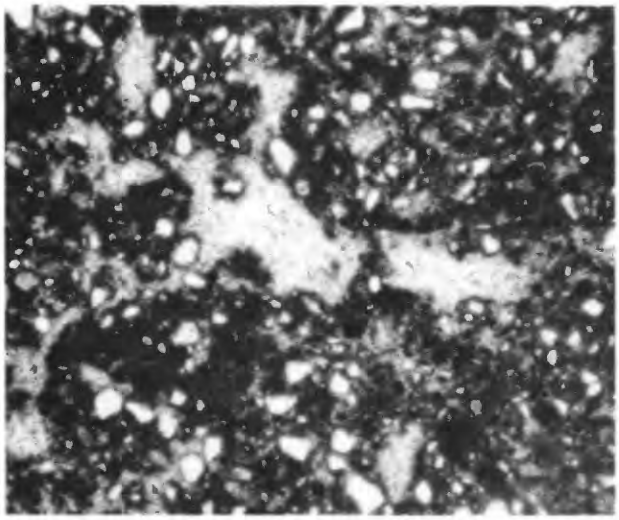

1 0 0.5mm

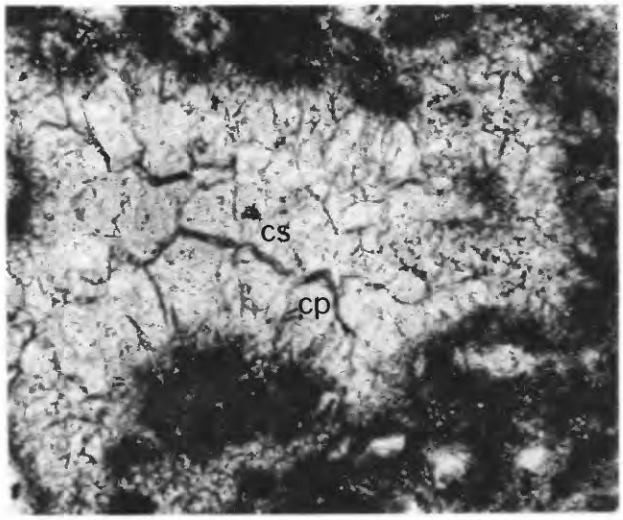

2 0 0.2mm

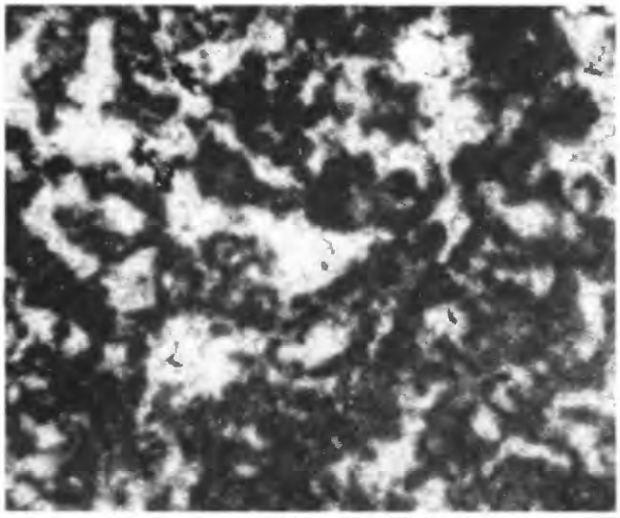

3 0 0.5mm

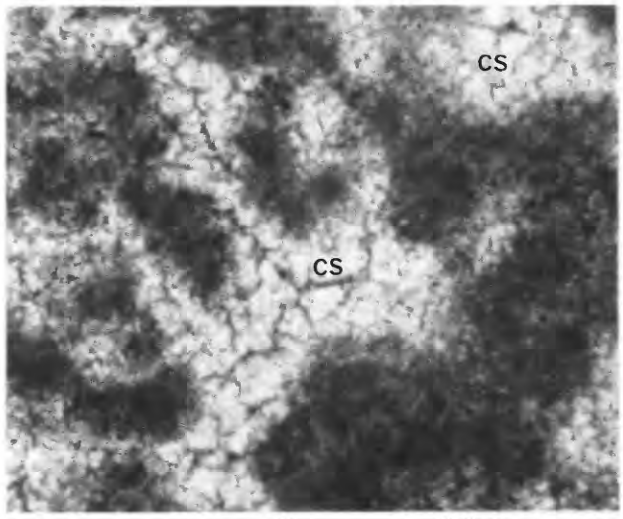

4 0 0.2mm

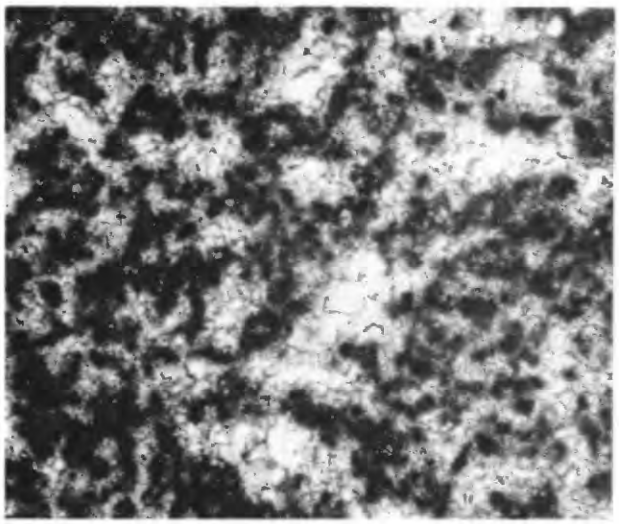

5 0 0.5mm

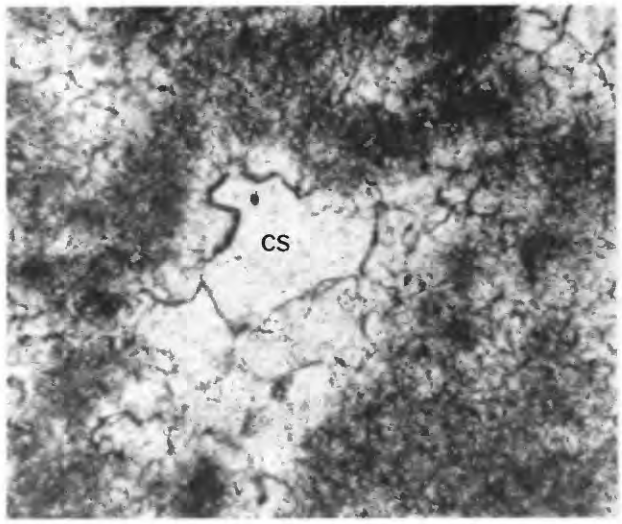

6 0 0.2mm

FENESTRATE PELOID PACKSTONE

PLATE 11

FIGURES 1–6. Algal oncolites; Hualapai Limestone Member, Grapevine Canyon.

1. Cut and polished surface of algal oncolites.
2, 3. 2, Transverse thin section of oncolites showing concentric banding. 3, Enlarged view of banding composed of fibrous calcite, wide light bands, and narrow dark concentric bands.
4. Scanning electron micrograph of algal oncolites, cavity lined with crystals of calcite.
5, 6. Cavity within oncolite lined with microcrystalline chert. 5, Polished and etched surface of algal oncolite illustrating small (5–10 μm) calcite rhombs and silica-lined cavity within banding. 6, Scanning electron micrograph of silica-lined cavity shown in figure 5.

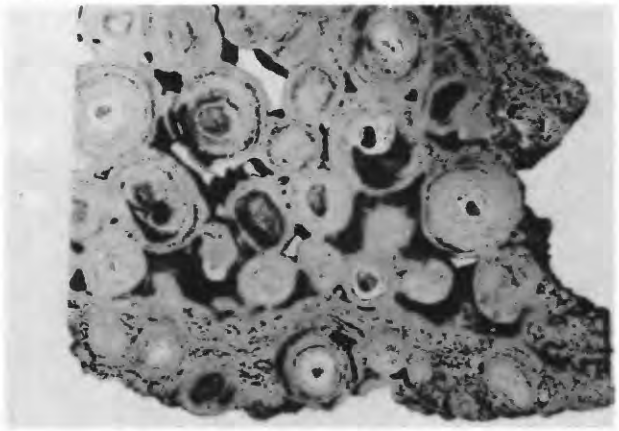

1 0 3cm

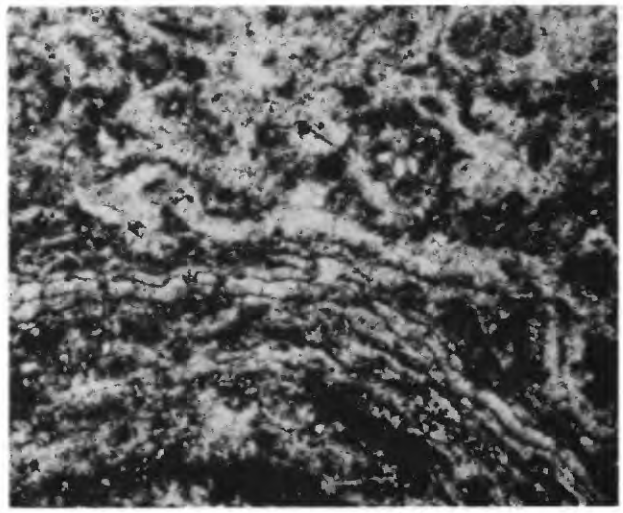

2 0 0.5mm

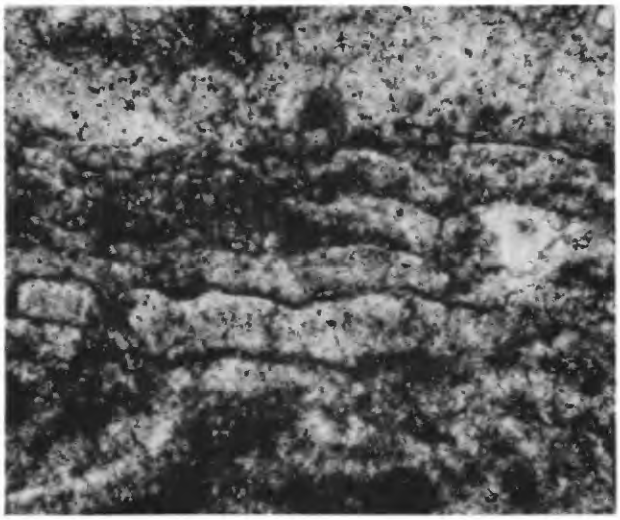

3 0 0.2mm

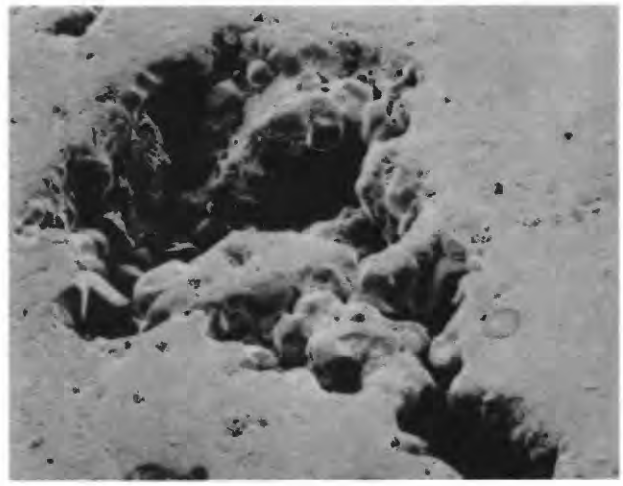

4 0 100μm

5 0 30μm

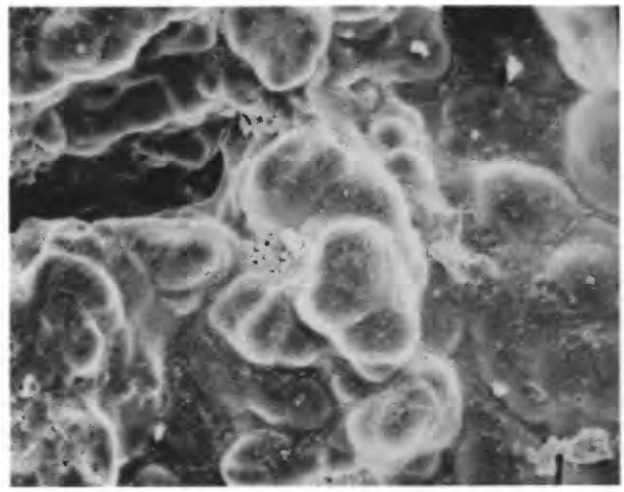

6 0 10μm

ALGAL ONCOLITES, GRAPEVINE CANYON

PLATE 12

FIGURES 1–6. *Juncus?* sp. indet. Specimen 876.

1, 2. Transverse section of stems of *Juncus?* sp. Dark areas are calcite preservation, light areas are opal.

3-6. Enlarged views of stems, showing plant wall and cell structure; fine details of plant structure are preserved by opal and jasper.

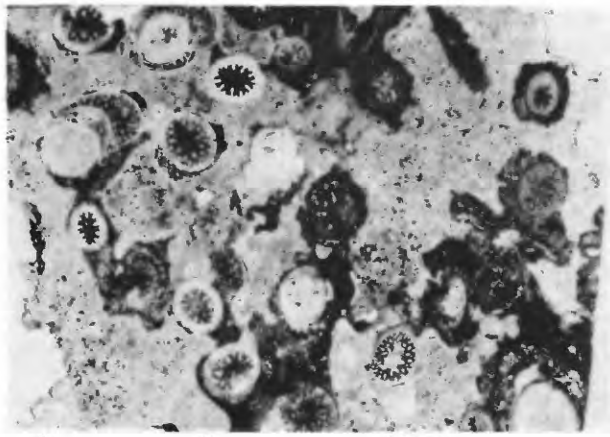

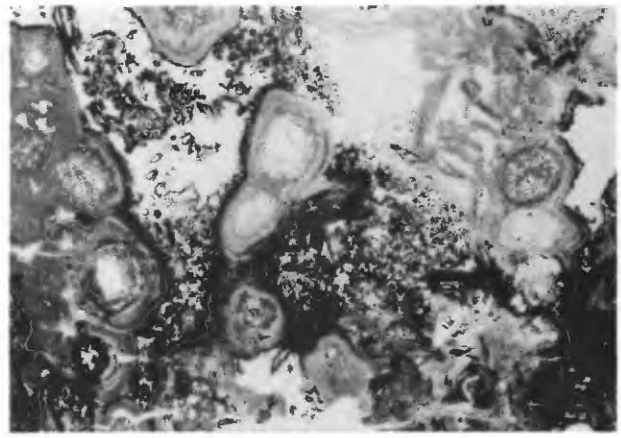

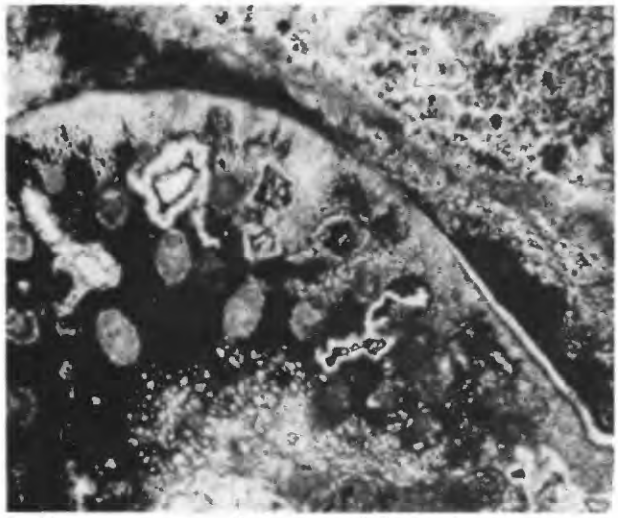

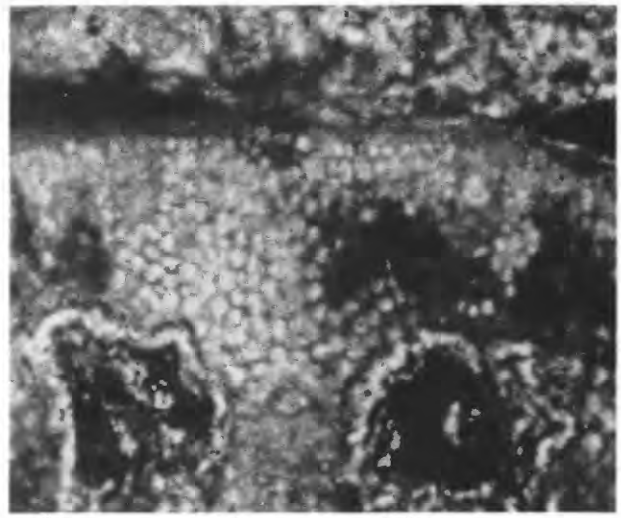

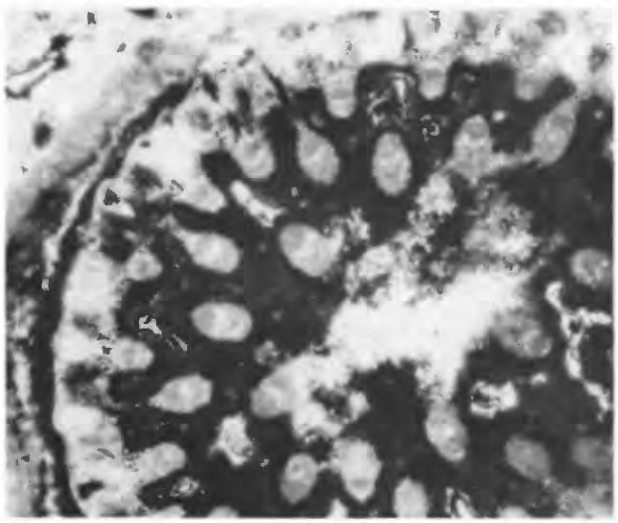

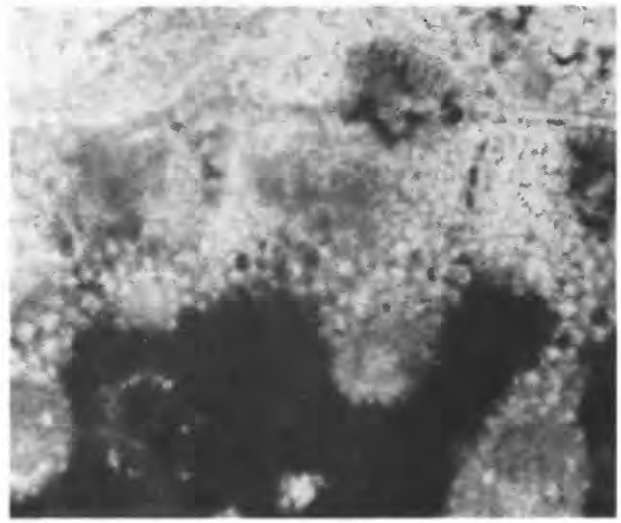

OPALIZED PLANT STEMS, *JUNCUS*? SP. INDET.

PLATE 13

FIGURES 1–6. Peloid packstones; Hualapai Limestone Member, Grapevine Canyon.

1. Peloid packstone; outlines of peloids are blurred. Peloids are 75–125 μm in size and composed of calcite crystals 5–10 μm in size. Specimen 800C.

2, 4, 6. Arenaceous peloid-pisoid-oncolitic packstone. Specimen 809. 2, Typical concentric-banded arenaceous pisoid. Quartz sand is subrounded, spaces between pisoids are composed of recrystallized micrite and contain quartz sand. 4, Enlarged view of pisoids, showing centers to be formed by peloids, and exterior by crudely banded concentric rings of micrite. Space in upper right of view is a void (V). 6, Enlarged view of area between peloids, showing space filled by sparry calcite (cs).

3. Peloid packstone, illustrating fuzzy outlines of peloids and sparry calcite (cs) filling of void between peloids. Specimen 800B.

5. Arenaceous peloid packstone. Photomicrograph shows sequence of diagenetic events. Formation of micritic peloids: deposition on peloids of first-phase calcite cement as stubby calcite crystals with pyramidal terminations growing at right angles to grain margins (cp); and final void filling by sparry calcite (cs). Specimen 800A.

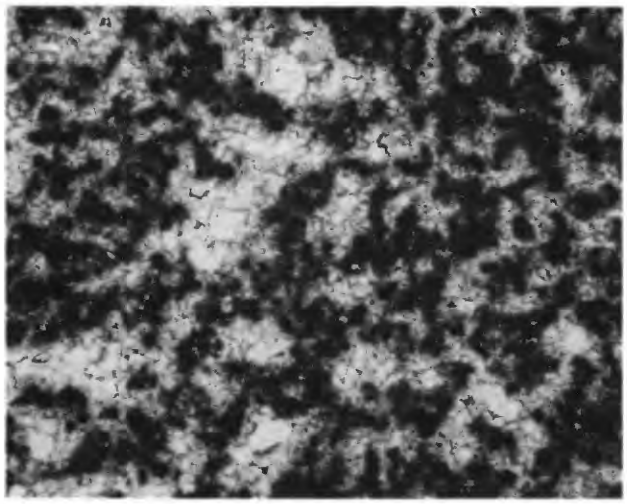

1 0 0.5mm

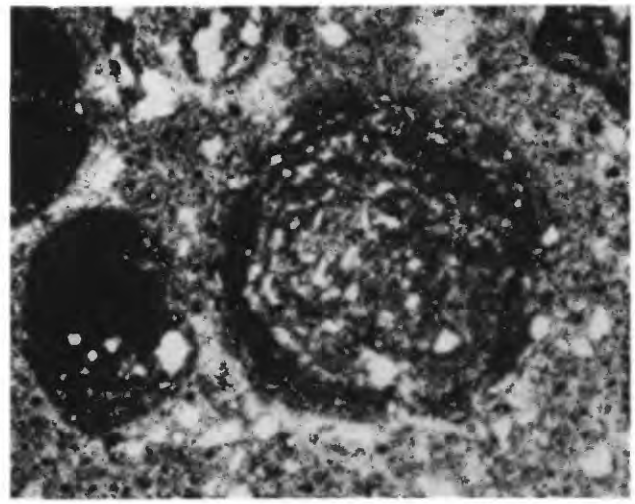

2 0 0.5mm

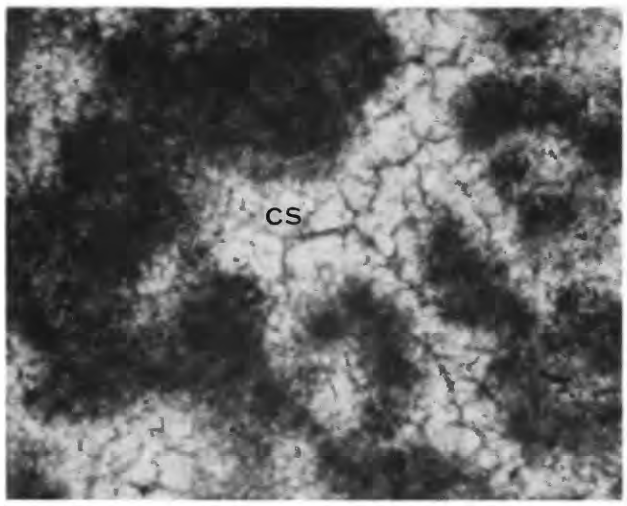

3 0 0.2mm

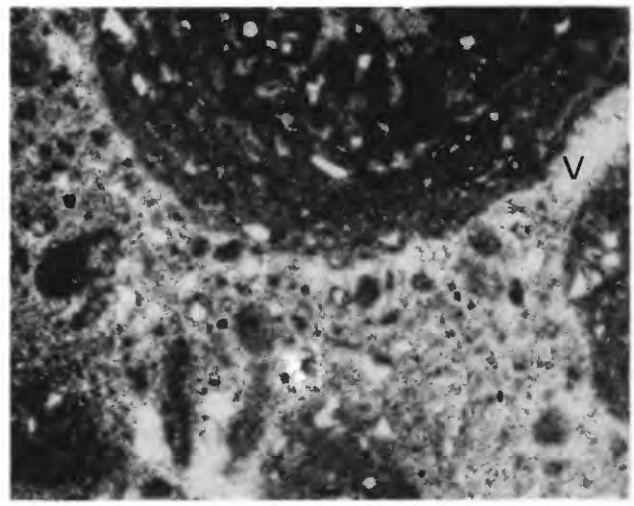

4 0 0.5mm

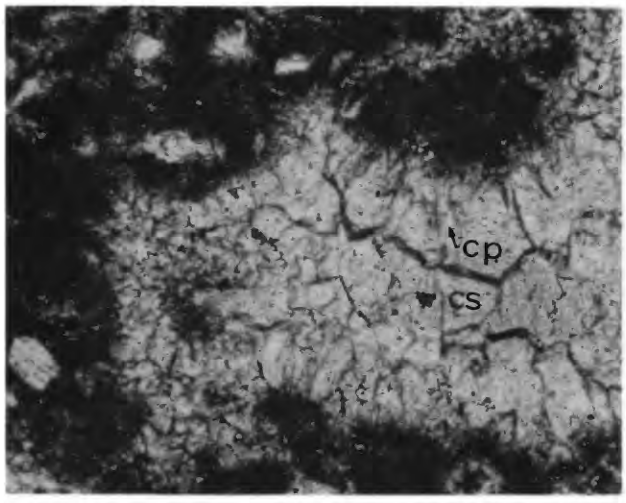

5 0 0.2mm

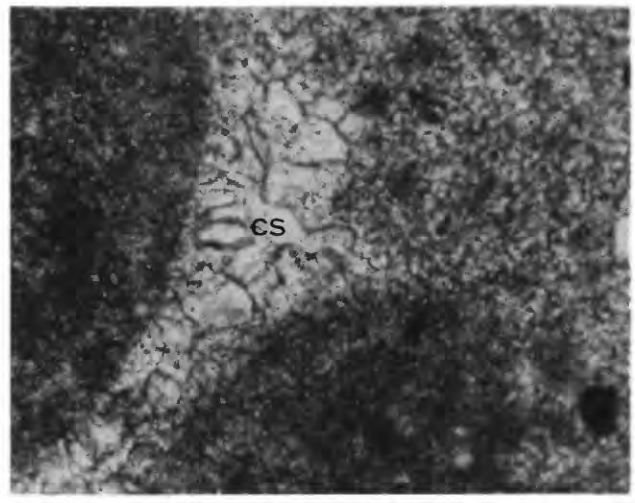

6 0 0.2mm

PELOID PACKSTONES

PLATE 14

FIGURES 1–6. Hualapai Limestone Member. First canyon north of Grapevine Canyon.

1. Dolomitic peloid packstone. Calcite crystal averages 100–125 μm in size, dark relict peloids are now inclusions within larger calcite crystals. Rock is porous. Dolomite rhombs are in cavity walls. Specimen 902.
2. Scanning electron micrograph of etched calcite surface. Calcite rhombs are 5–10 μm in size. Specimen 903.
3. Peloid packstone. Crossed nicols. Black areas are pores. Elongate gray peloids are composed of 4 μm-size calcite crystals. White areas are sparry calcite fillings. Specimen 904.

4, 5. 4, Arenaceous peloid-mudlump packstone. Crossed nicols. Mudlump and peloids show evidence of two periods of cementation; band of gray radiaxial cement lines each particle (cr), followed by sparry calcite (cs) void-filling cement. 5, Scanning electron micrograph of mudlump. Gray areas are 1–4 μm calcite rhombs; linear white material is clay. Specimen 908.

6. Arenaceous peloid-mudlump packstone. Crossed nicols. Cemented by sparry calcite (cs) and radiaxial calcite.

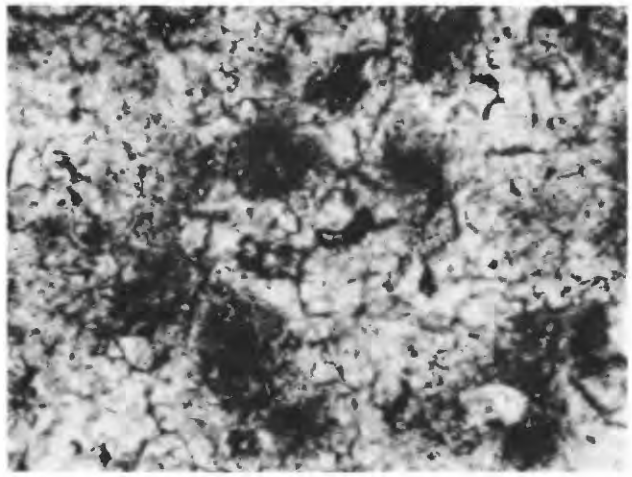

1 0 0.2mm

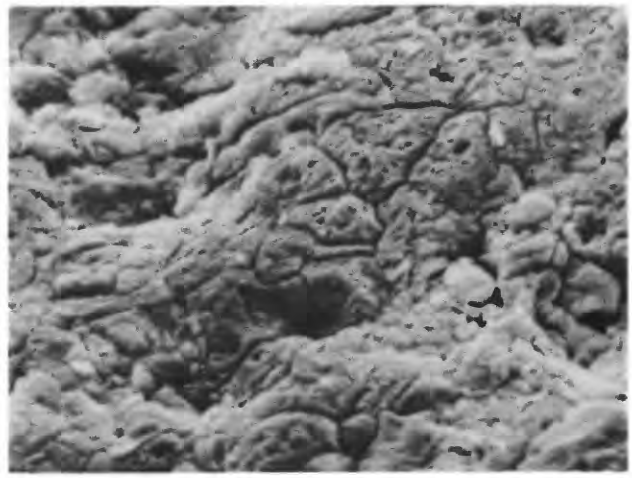

2 0 10μm

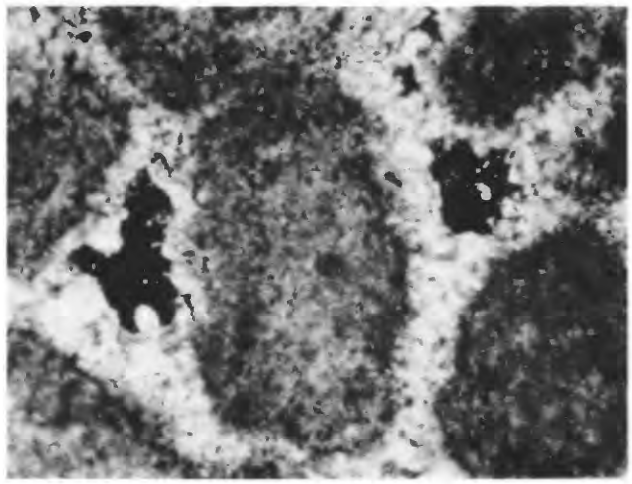

3 0 0.2mm

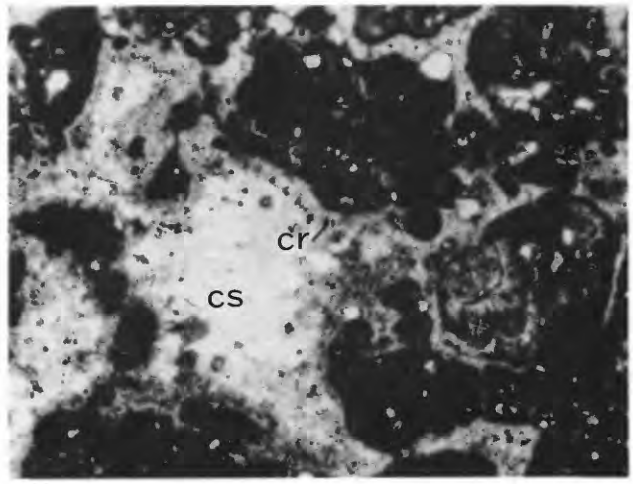

4 0 0.5mm

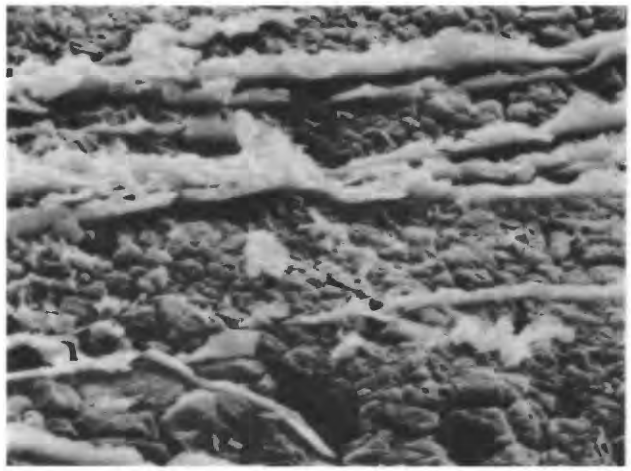

5 0 3μm

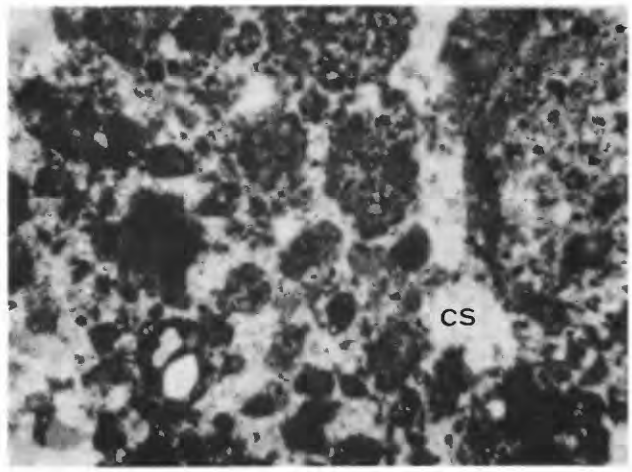

6 0 0.5mm

SPECIMENS FROM NORTH OF GRAPEVINE CANYON

PLATE 15

FIGURES 1–6. Hualapai Limestone Member. First canyon north of Grapevine Canyon.

1. Arenaceous peloid-mudlump packstone. Voids are filled by sparry calcite (cs). Specimen 910.

2, 3. 2, Fenestrate arenaceous peloid-mudlump packstone. Quartz sand grains (Q) are subangular to subrounded. Void between micritic particles is now filled by two generations of calcite; vadose silt composed of fine crystalline calcite (vs) and later sparry (cs) void filling. 3, Micrite envelope? (me) filled by sparry calcite (cs) in microspar matrix. Micrite envelope may represent former aragonite mudlump. Specimen 911.

4, 5. 4, Vuggy arenaceous peloid-mudlump packstone to lime mudstone. Sequence of vug filling is two distinct bands of radiaxial fibrous calcite (cr_1, cr_2) and void filling by sparry calcite (cs). 5, Enlarged view of small vug, showing micrite matrix (cm), two bands of light and dark radiaxial fibrous cement (cr_1, cr_2), and final sparry calcite (cs) void filling.

6. Vuggy arenaceous peloid-mudlump-lime mudstone. Microfabric is dark micrite matrix (cm), quartz sand (Q), and sparry calcite (cs) vuggy filling. Specimen 912.

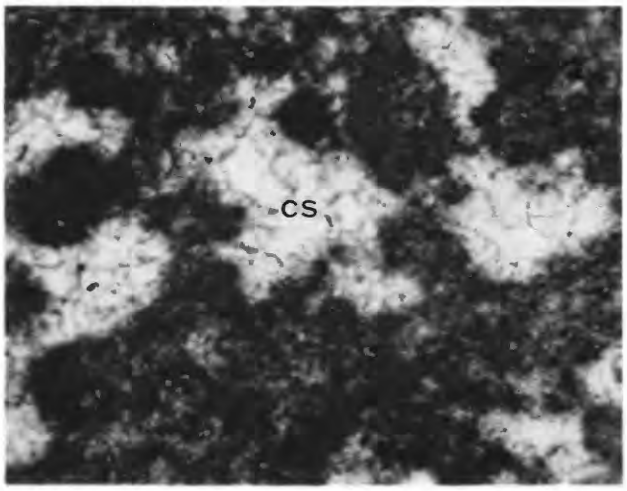

1 0 0.2mm

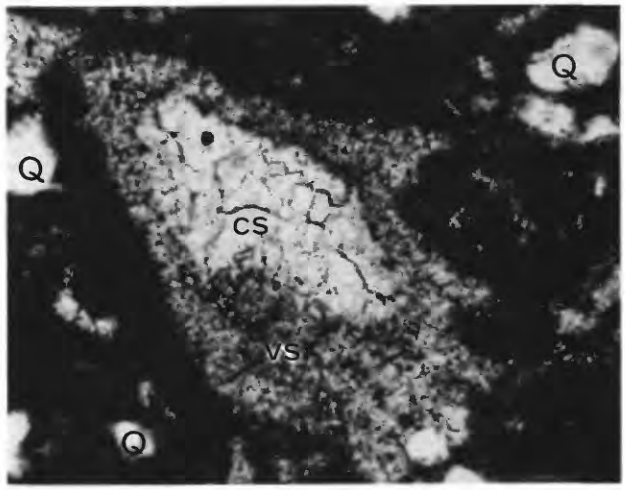

2 0 0.2mm

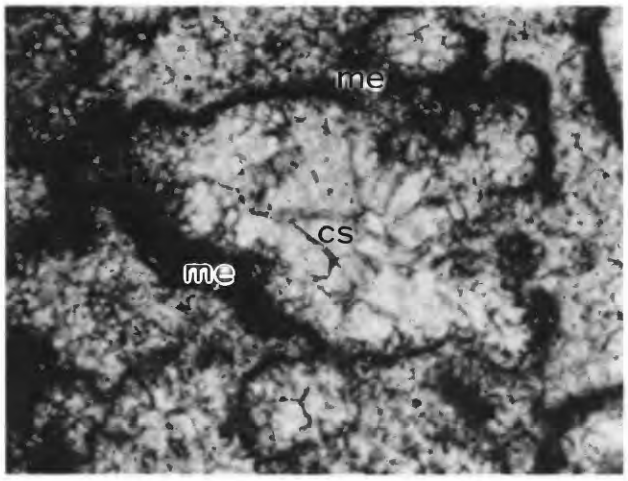

3 0 0.2mm

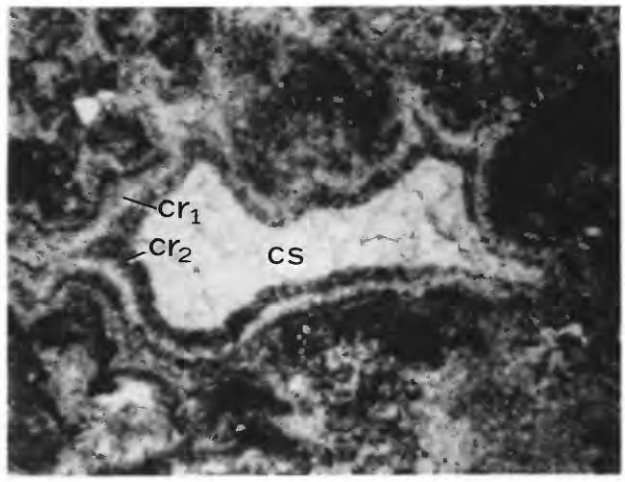

4 0 0.5mm

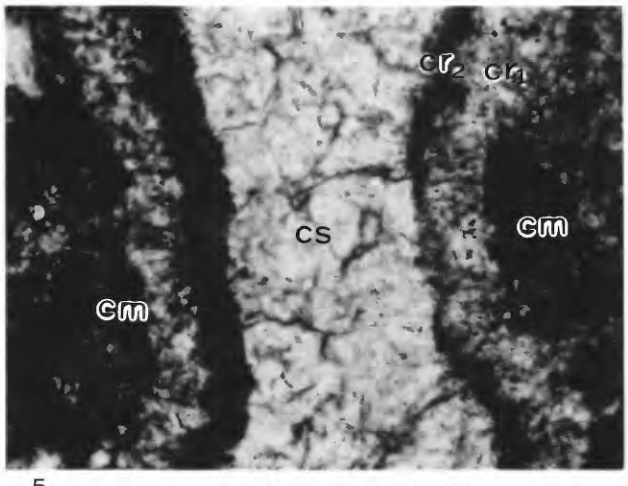

5 0 0.2mm

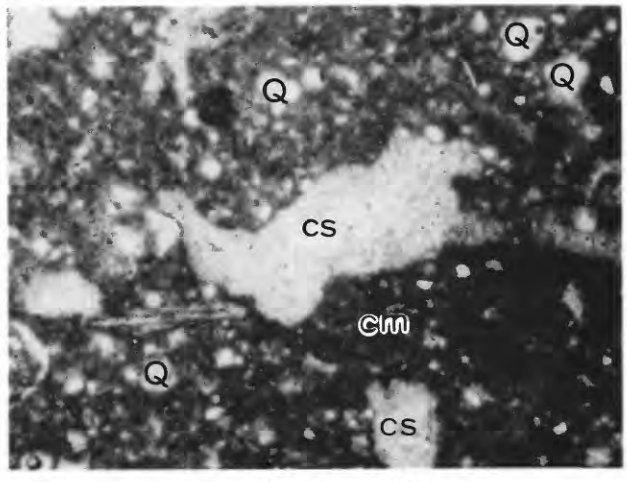

6 0 0.5mm

SPECIMENS FROM NORTH OF GRAPEVINE CANYON

PLATE 16

FIGURES 1–6. Hualapai Limestone Member. First canyon north of Grapevine Canyon.

1–3. Peloid-mudlump packstone. Photomicrograph shows particle size, peloid to pisolitic configuration of micritic particles, and possible vadose silt (vs); area between particles is filled by sparry calcite (cs). Specimen may represent ancient caliche. 2, Enlarged view between micritic particles shows long slender calcite (cr) crystals and final sparry calcite (cs) void filling. 3, Scanning electron micrograph of etched micritic surface. Quartz sand (Q) grain in center of view is surrounded by calcite crystals. Specimen 913.

4–6. Fenestrate arenaceous peloid-mudlump packstone to lime mudstone with sparry calcite void filling. 4, Abundant subrounded quartz sand grains (Q), sparry calcite (cs), and irregular voids (V). 5, Details of void fillings, showing early stage radiaxial fibrous (cr) cement followed by sparry calcite (cs) void filling. 6, Scanning electron micrograph showing quartz grain (Q) within micrite. Calcite crystals within micrite are only 2–4 μm in size. Specimen 914.

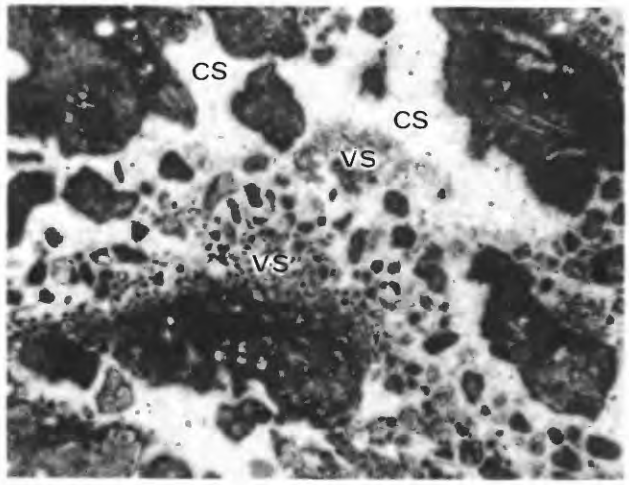

1

0 0.5μm

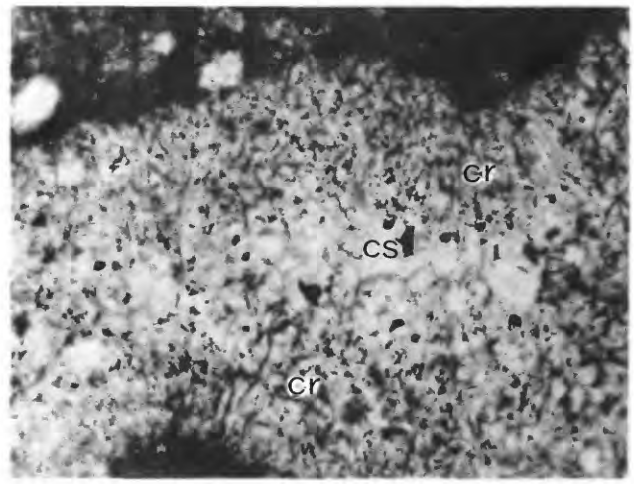

2

0 0.2mm

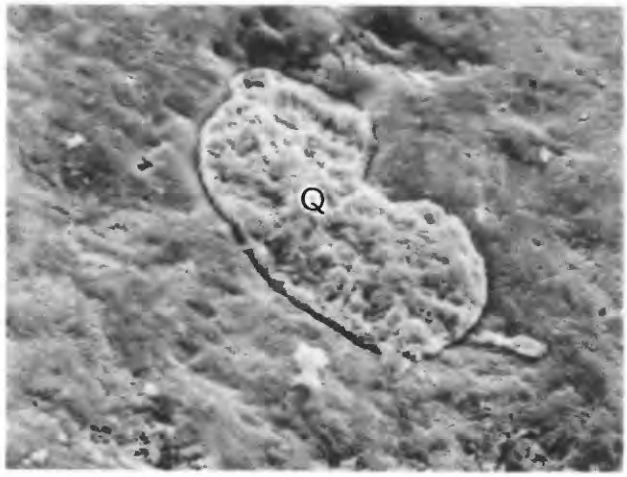

3

0 20μm

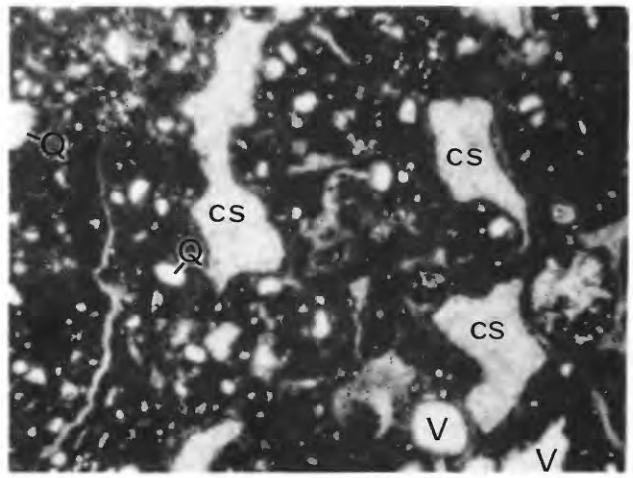

4

0 0.5mm

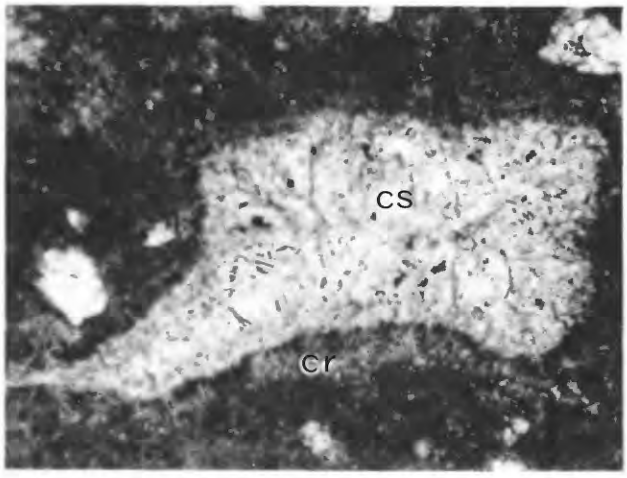

5

0 0.5mm

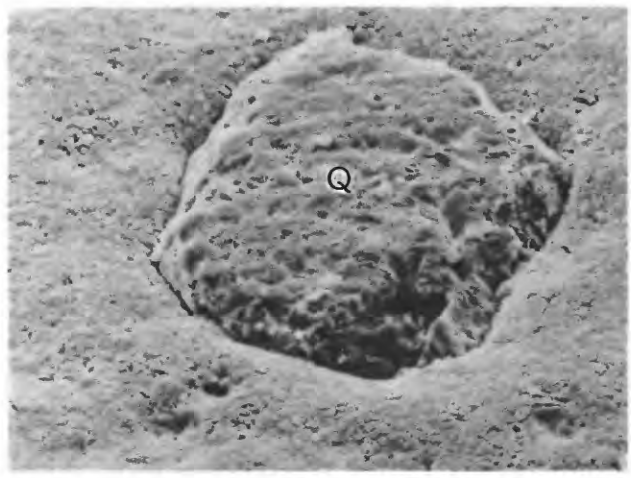

6

0 30μm

SPECIMENS FROM NORTH OF GRAPEVINE CANYON

PLATE 17

FIGURES 1–6. Hualapai Limestone Member. First canyon north of Grapevine Canyon.

1–3. Arenaceous peloid-lime mudlump oncolitic packstone. 1, Left half of view shows irregular banded or circular objects, which are believed to be of algal origin; but interior of circular objects is made of arenaceous compound mudlumps and peloids. Right half of view shows poorly defined peloids, quartz grains (Q), and micritic matrix. 2, Enlarged view of small cavity filled by sparry calcite (cs). Micritic matrix contains quartz grains (Q). 3, Scanning electron micrograph of etched surface of micrite. Linear white bands in center of view are concentrations of clay minerals. Clays are relatively abundant between calcite rhombs.

4–6. Arenaceous lime mudstone. 4, Cross section of ostracode filled by sparry calcite and surrounded by micrite. 5, 6, Scanning electron micrographs. 5, Linear fractures or stylolites filled by clay minerals. 6, Detailed view of micrite calcite crystals in 1–4-μm size range, white objects between calcite crystals are clay (cy) minerals. Specimen 916.

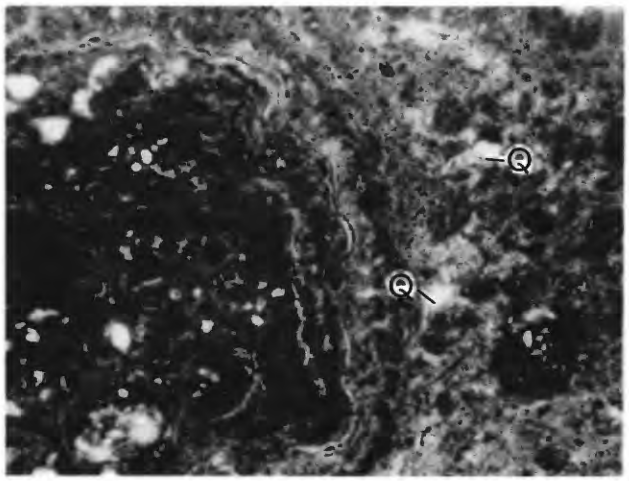

1 0 0.5mm

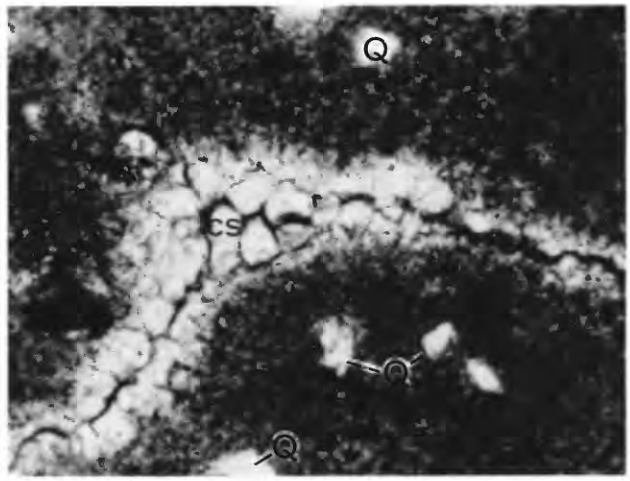

2 0 0.2mm

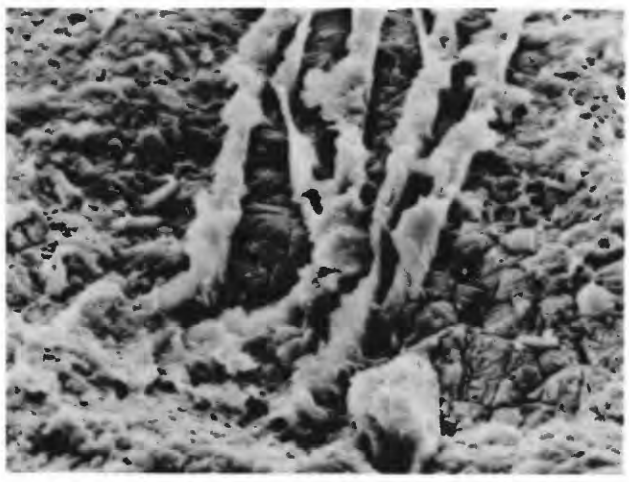

3 0 10μm

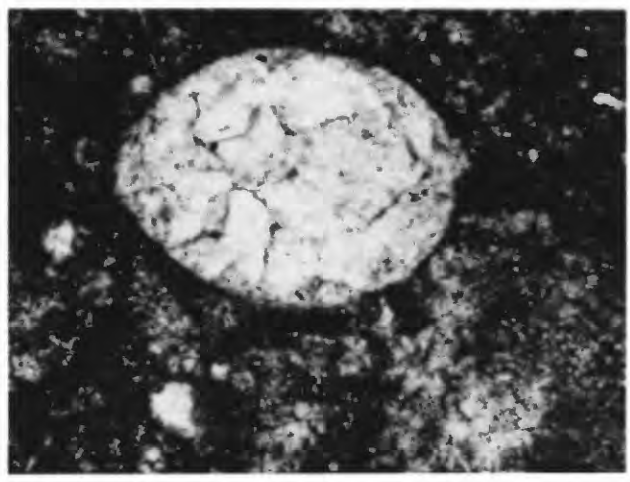

4 0 0.2mm

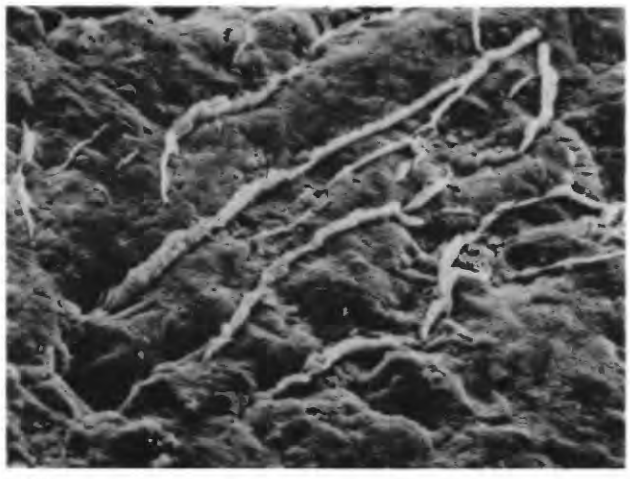

5 0 10μm

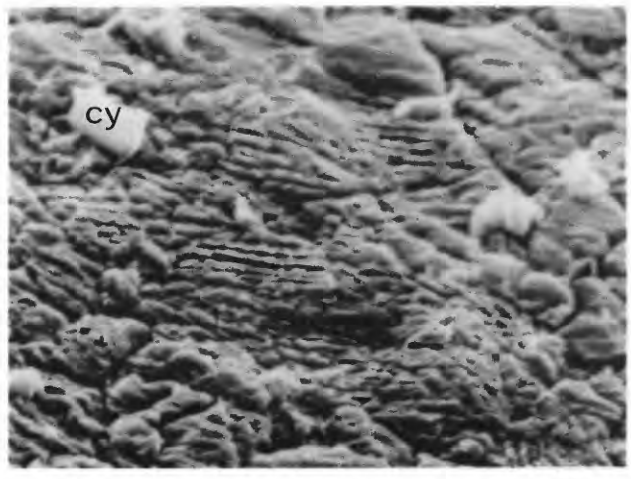

6 0 3μm

SPECIMENS FROM NORTH OF GRAPEVINE CANYON

PLATE 18

FIGURES 1–6. Hualapai Limestone Member. First canyon north of Grapevine Canyon.

1–3. Fenestrate arenaceous peloid-mudlump-oncolitic packstone. 1, Quartz grains (Q) are subrounded and in micritic matrix. Straight object (1s) in center of mudlump may be molluscan fragment, on which algal lamination grew. 2, Details of irregular-shaped oncolite, which has center formed by peloids and quartz sand. Algal laminations are seen on outer parts. Two stages of void filling can be seen. Radiaxial cement (cr), 100–300 μm wide and a final void-filling sparry calcite (cs). 3, Details of void filling, dark micritic matrix (cm), radiaxial calcite (cr), and final void-filling sparry calcite cement (cs). Long-axial fibrous cement is well displayed under polarizing microscope. Specimen 918.

4–6. Specimen 892C. 4, Algal oncoids and platy laths of calcite set in sparry calcite cement. 5, Algal oncoids in lower left side (ao) and platy laths in upper part of view. Sparry calcite cement (cs) and void space (V). 6, Algal oncolites (ao); note large platy lath (pl) at extreme left of view and dark central band in lath; voids are filled by sparry calcite (cs).

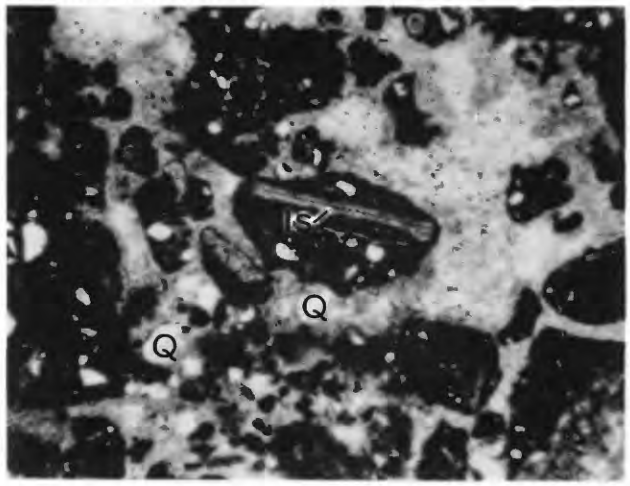

1 0 0.5mm

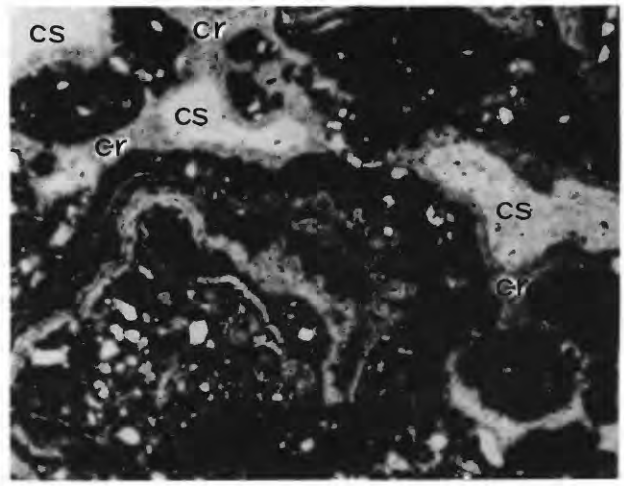

2 0 0.5mm

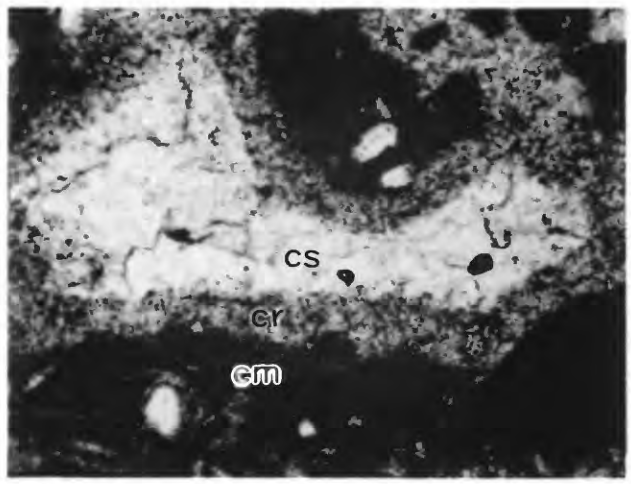

3 0 0.2mm

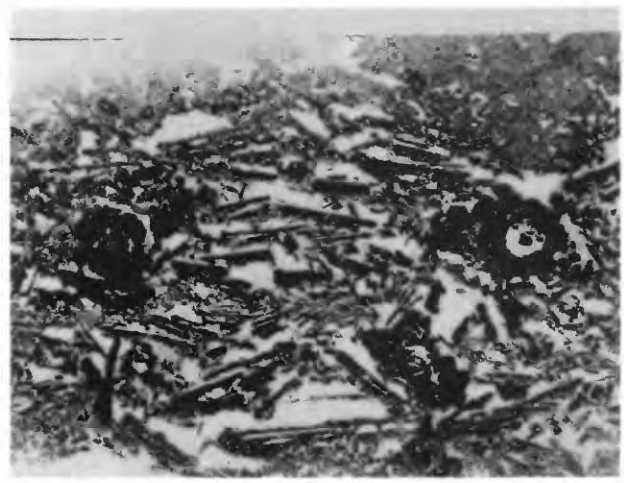

4 0 10mm

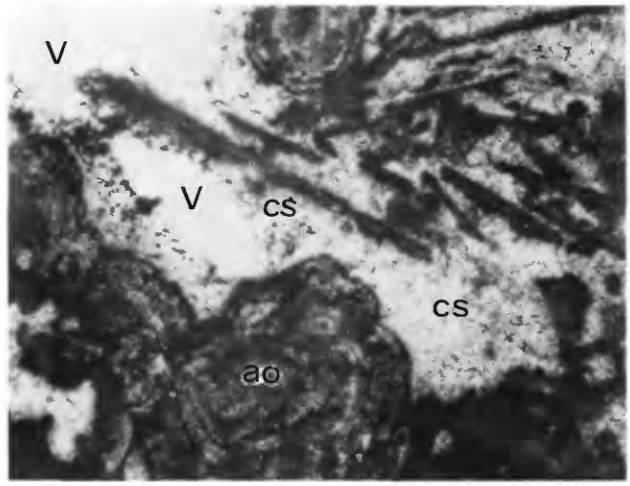

5 0 0.5mm

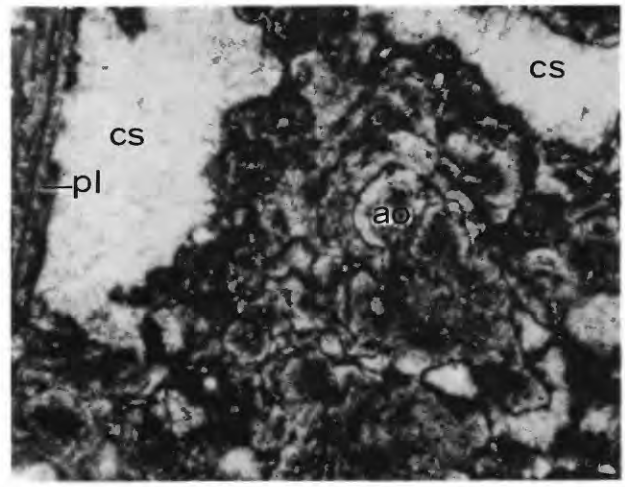

6 0 0.5mm

SPECIMENS FROM NORTH OF GRAPEVINE CANYON

PLATE 19

FIGURES 1–6. Hualapai Limestone Member. First canyon north of Grapevine Canyon.

1. Radiaxial fibrous calcite, filling void in arenaceous pellet-mudlump-lime mudstone. Marginal portion of radiaxial fibrous mosaic exhibits preferred elongation and crystallographic orientation of crystals normal to micritic substrate. Numerous inclusion zones can be observed in fibrous crystals. Text figure 7 illustrates crystal sizes and inclusion patterns found in this specimen. Specimen 908.

2–4. Arenaceous peloid-algal-oncolitic packstone to grainstone. Crossed nicols. 2, Right half of view shows dark and light laminations of large algal oncolite with quartz sand inclusions (Q). 4, Arenaceous mudlump and algal oncolites. Light and dark bands of algal oncolites are seen in right third of view. Radiaxial fibrous calcite filling can be observed (cr) between mudlumps and algal oncolites. Specimen 918.

3. Radiaxial fibrous calcite (crossed nicols) that appears to have developed on a micritic envelope. Interiors of micritic envelope filled with sparry calcite (cs). Inclusion zone (iz) is more or less parallel with micrite substrate. Specimen 911.

5–6. Arenaceous pellet-mudlump packstone to grainstone. 5, Radiaxial fibrous calcite void filling. Plane light. 6, Specimen shows marginal portions of radiaxial fibrous mosaic with preferred elongation and crystallographic orientation normal to substrate. Crossed nicols. Specimen 914.

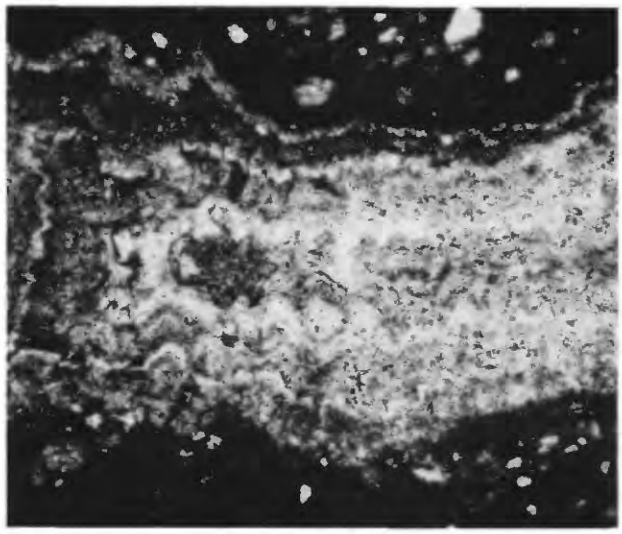

1 0 0.5mm

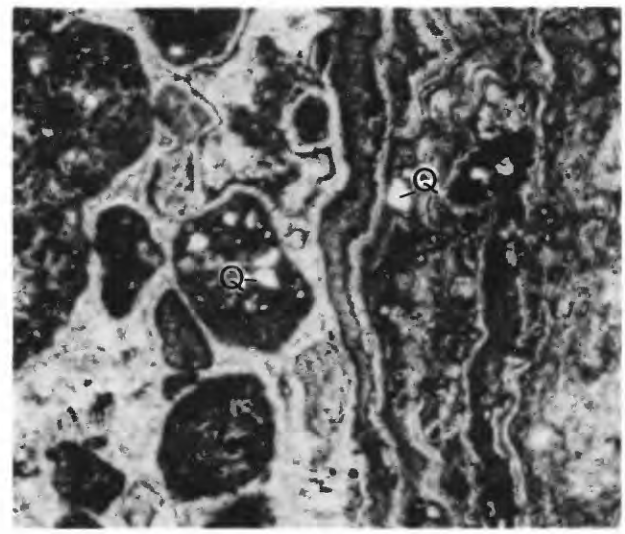

2 0 0.5mm

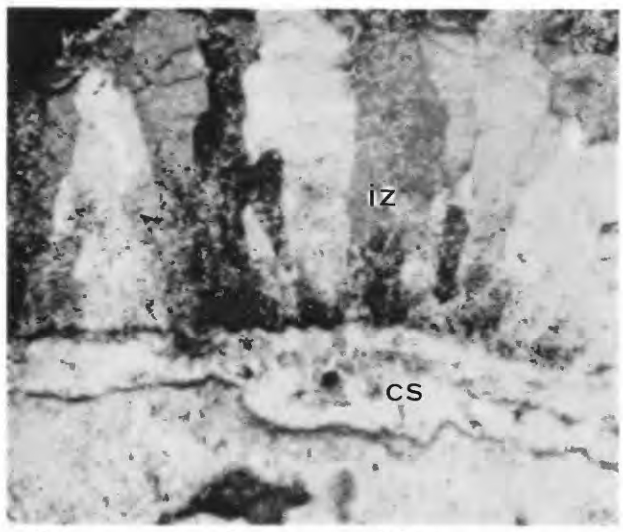

3 0 0.2mm

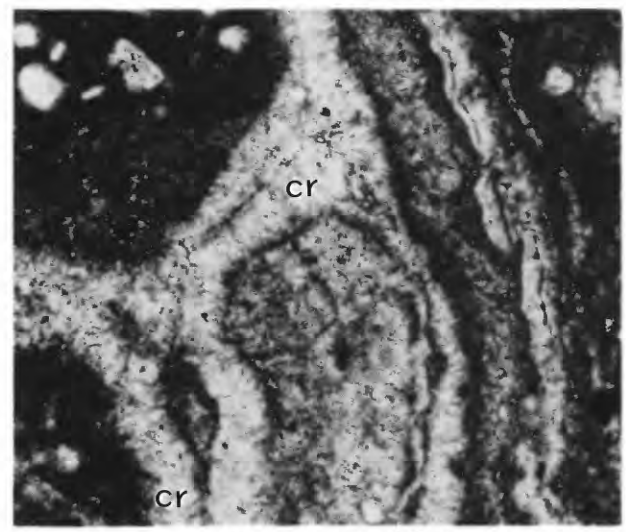

4 0 0.2mm

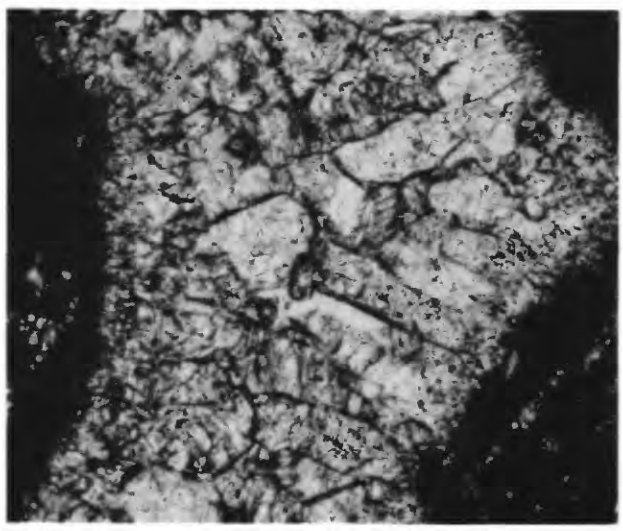

5 0 0.2mm

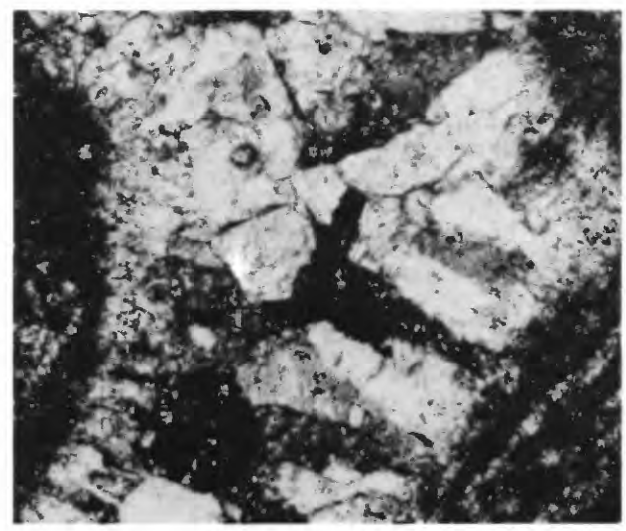

6 0 0.2mm

SPECIMENS FROM NORTH OF GRAPEVINE CANYON